

2023-02

Applying landscape metrics to species distribution model predictions to characterize internal range structure and associated changes

Curd, A

<http://hdl.handle.net/10026.1/20403>

10.1111/gcb.16496

Global Change Biology

Wiley

All content in PEARL is protected by copyright law. Author manuscripts are made available in accordance with publisher policies. Please cite only the published version using the details provided on the item record or document. In the absence of an open licence (e.g. Creative Commons), permissions for further reuse of content should be sought from the publisher or author.

Applying landscape metrics to species distribution model predictions to characterise internal range structure and associated changes

Running Title: “Better species range characterisation”

Amelia Curd^{1✉*}, Mathieu Chevalier^{1✉*}, Mickaël Vasquez¹, Aurélien Boyé¹, Louise B. Firth², Martin P. Marzloff¹, Lucy M. Bricheno³, Michael T. Burrows⁴, Laura E. Bush⁵, Céline Cordier¹, Andrew J. Davies^{6,7}, J. A. Mattias Green⁸, Stephen J. Hawkins^{2,9,10}, Fernando P. Lima^{11,12}, Claudia Meneghesso^{11,12,13}, Nova Mieszkowska^{10,14}, Rui Seabra¹¹ and Stanislas F. Dubois¹

¹ IFREMER, Centre de Bretagne, DYNECO LEBCO, 29280 Plouzané, France.

² School of Biological and Marine Sciences, University of Plymouth, Drake Circus, Plymouth, PL4 8AA, United Kingdom.

³ National Oceanography Centre, Joseph Proudman Building, 6 Brownlow Street, Liverpool, L3 5DA, UK.

⁴ Scottish Association for Marine Science, Scottish Marine Institute, Oban, PA37 1QA, UK.

⁵ FUGRO GB Marine Limited, Gait 8, Research Park South, Heriot-Watt University, Edinburgh EH14 4AP, UK.

⁶ Department of Biological Sciences, University of Rhode Island, Kingston, RI 02881, USA.

⁷ Graduate School of Oceanography, University of Rhode Island, Narragansett, RI 02882, USA.

⁸ School of Ocean Sciences, Bangor University, Askew Street, Menai Bridge, LL59 5AB Bangor, United Kingdom.

⁹ Ocean and Earth Science, University of Southampton, National Oceanography Centre Southampton, Waterfront Campus, European Way, Southampton SO14 3ZH, UK

¹⁰ The Marine Biological Association of the UK, Citadel Hill, Plymouth, PL1 2PB, UK

¹¹ CIBIO, Centro de Investigação em Biodiversidade e Recursos Genéticos, InBIO Laboratório Associado, Campus de Vairão, Rua Padre Armando Quintas, nº 7, 4485-661 Vairão, Portugal

¹² BIOPOLIS Program in Genomics, Biodiversity and Land Planning, Campus de Vairão, Rua Padre Armando Quintas, nº 7, 4485-661 Vairão, Portugal

¹³ Departamento de Biologia, Faculdade de Ciências da Universidade do Porto, R. Campo Alegre, s/n, 4169-007 Porto, Portugal

¹⁴ Department of Earth, Ocean and Ecological Sciences, School of Environmental Sciences, University of Liverpool, Nicholson Building, Brownlow Street, Liverpool, L69 3GP, UK

*Amelia Curd and Mathieu Chevalier should be considered joint first author

✉ E-mail: amelia.curd@ifremer.fr

Abstract

Distributional shifts in species ranges provide critical evidence of ecological responses to climate change. Assessments of climate-driven changes typically focus on broad-scale range shifts (e.g. poleward or upward), with ecological consequences at regional and local scales commonly overlooked. While these changes are informative for species presenting continuous geographic ranges, many species have discontinuous distributions - both natural (e.g. mountain or coastal species) or human-induced (e.g. species inhabiting fragmented landscapes) - where within-range changes can be significant. Here, we use an ecosystem engineer species (*Sabellaria alveolata*) with a naturally fragmented distribution as a case study to assess climate-driven changes in within-range occupancy across its entire global distribution. To this end, we applied landscape ecology metrics to outputs from species distribution modelling (SDM) in a novel unified framework. SDM predicted a 27.5% overall increase in the area of potentially suitable habitat under RCP 4.5 by 2050, which taken in isolation would have led to classify the species as a climate change winner. SDM further revealed that the latitudinal range is predicted to shrink because of decreased habitat suitability in the equatorward part of the range, not compensated by a poleward expansion. The use of landscape ecology metrics provided additional insights by identifying regions that are predicted to become increasingly fragmented in the future, potentially increasing extirpation risk by jeopardising metapopulation dynamics. This increased range fragmentation could have dramatic consequences for ecosystem structure and functioning. Importantly, the proposed framework - which brings together SDM and landscape metrics - can be widely used to study currently overlooked climate-driven changes in species internal range structure, without requiring detailed empirical knowledge of the modelled species. This approach represents an important advancement beyond

predictive envelope approaches and could reveal itself as paramount for managers whose spatial scale of action usually ranges from local to regional.

Keywords (6-10 words or phrases)

Climate change | Range fragmentation | Engineer species | Species distribution modelling
| Landscape metrics | Within-range structure | Patch dynamics

| INTRODUCTION

Geographic distributions of species are determined by complex interactions and feedbacks between climate, ecological and evolutionary processes (Parmesan and Yohe, 2003; Burrows et al., 2020; Paquette and Hargreaves, 2021). Several pioneering studies have shown the profound implications of climate-driven modification on assemblage composition, community structure and ecosystem functioning (Pecl et al., 2017; Walther, 2010). Under future climate conditions, the geographic ranges of many species are predicted to shift in size, latitude, depth and/or elevation (Poloczanska et al., 2016; Pinsky et al., 2020). Such changes have typically been documented for either the leading poleward or trailing equatorward range edges (i.e. the external range structure), thus overlooking changes taking place within ranges (i.e. the internal range structure; Csörgő et al., 2020).

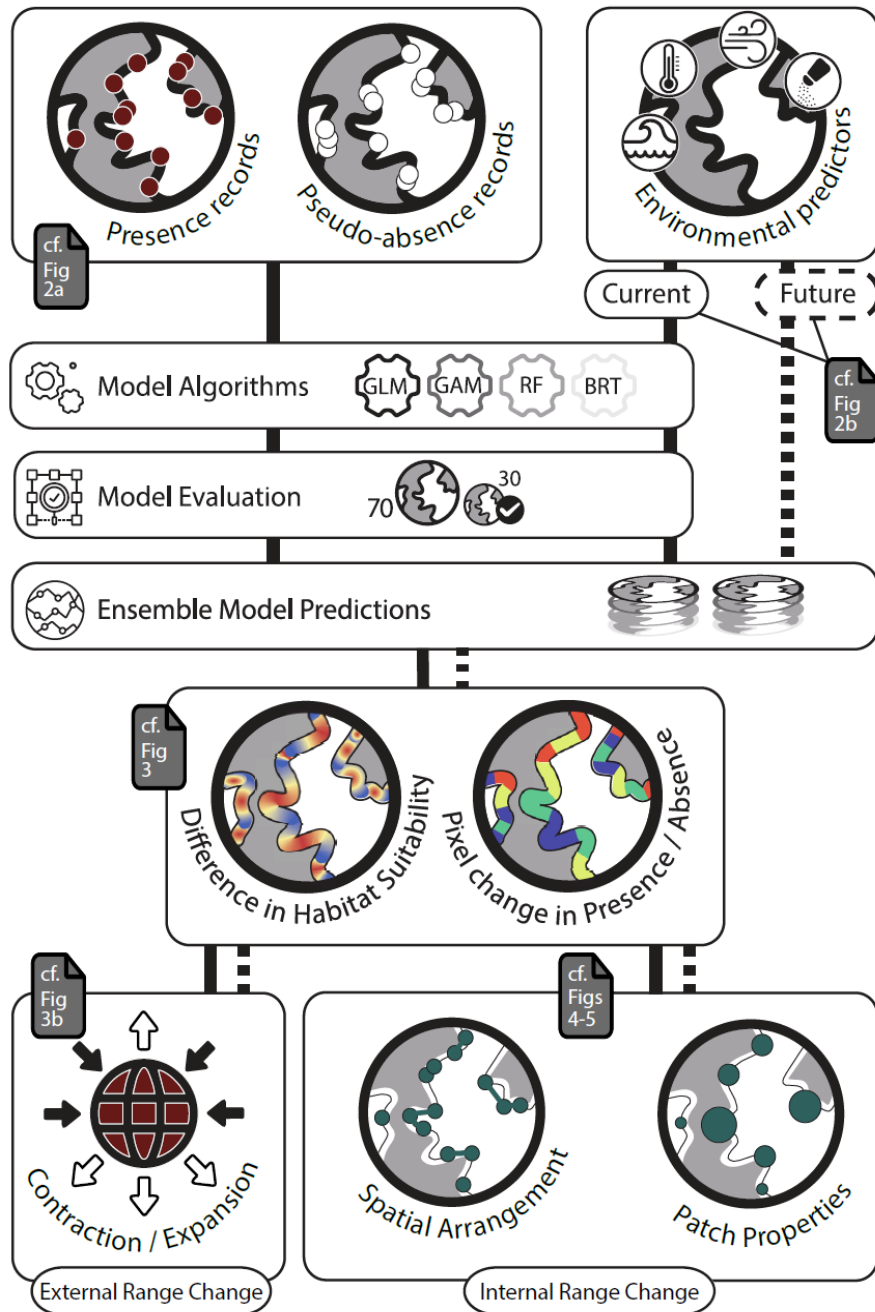


FIGURE 1. Modelling framework bringing together SDM outputs and landscape metrics. SDMs were fitted on spatially thinned presence records and randomly-generated

pseudo-absences (see Figure 2a). Six environmental predictors: minimum air temperature, maximum sea surface temperature, fetch, salinity, wave height and tidal amplitude (see Figure 2b) were used to explain the species spatial distribution. Four algorithms were selected to build the models: GLM (generalized linear models), GAM (generalized additive models), RF (random forests) and BRT (boosted regression trees). We used an ensemble model approach to predict and map the current and the future habitat suitability across the species latitudinal range. Habitat suitability is defined as the likelihood of occurrence of a species in association with environmental variables. Ensemble predictions were then binarised into presence/absence (P/A) maps. These P/A maps were then used to (1) evaluate changes in range size and distribution shifts (see Figure 3b) and (2) compute various landscape metrics using both current and future P/A predictions. The landscape metrics were then used to study the spatial arrangement of predicted patches of P/A within the species range over time (Figures 4-5). Note that we applied landscape metrics to outputs from the ensemble model, however this approach can be applied separately to each model output in order to obtain information regarding the influence of pseudo-absence datasets, model runs and algorithms on internal range change metrics.

Perhaps this omission betrays the implicit assumption that species distributions are spatially continuous (e.g. most IUCN polygons are continuous; Rocchini et al., 2011). Under this supposition, focusing on measuring changes in the external range structure such as changes in range size (Pither, 2003; Thomas, 2012), or quantifying the velocity at which the range centroid and/or margins (trailing and leading edges) may shift in the future may suffice (Sunday et al., 2012; Lenoir et al., 2020; Fredston-Hermann et al., 2020). However, by relying only on external metrics, these broad-scale studies overlook the changes that can take place within ranges and which ultimately determine the abundance, occurrence and connectivity of local populations (VanDerWal et al., 2013). For instance, regional

persistence of rare species, or those living in fragmented landscapes such as mountainous, coastal or degraded areas, usually present discontinuous distributions that rely on complex networks of interconnected populations whose responses to climate-driven changes cannot be accurately assessed using metrics characterising broad-scale patterns in biogeographical distribution changes (Opdam & Wascher, 2004; Mestre et al., 2017). In such cases, quantifying changes in the internal structure of geographical ranges is critical for understanding species vulnerability to climate change. For instance, range fragmentation can increase local extinction risk by jeopardising metapopulation dynamics (Mestre et al., 2017). To illustrate this point, we focused on the naturally discontinuous distribution of an intertidal ecosystem engineer, the reef-building honeycomb worm *Sabellaria alveolata* (Linnaeus, 1767).

Intertidal ecosystems - and engineered intertidal habitats in particular - support high biodiversity and deliver important ecosystem services to society such as protection from erosion and flooding, water quality, food resources (shellfish, seaweeds), sites for aquaculture and fish nursery grounds (Barbier et al., 2011). These ecosystems are however facing strong pressures, being under the influence of multiple stressors acting at multiple scales (regional and local) whose effect on biodiversity can be reinforced by climate change (Bugnot et al., 2021). Moreover, intertidal species are exposed to both terrestrial and marine environmental conditions, which remain challenging to account for (Helmuth et al., 2006). Taking advantage of extensive occurrence records (Curd et al., 2020), coupled with fit-for-purpose resolution (0.083 decimal degrees,) current and future climatologies of marine and terrestrial conditions, we developed a species distribution model (SDM) to

predict the current and future distribution of *S. alveolata* across its full global latitudinal range (32-61° N). We then assessed how the external and internal range structure of *S. alveolata* will be altered in response to climate change. The latter was assessed by making novel use of landscape metrics applied to SDM outputs.

Landscape ecology is a discipline all unto itself (Turner et al. 2005). A great variety of landscape composition (e.g., the number and amount of different habitat types) and configuration (the spatial arrangement of those classes) metrics have been developed for categorical data (Lausch et al., 2015). These metrics make it possible to improve our understanding of, for example, the effect of landscape complexity on biodiversity (Schindler et al., 2013) or habitat connectivity on metapopulation dynamics (Howell et al., 2018). The cornerstone of our approach is to have transformed species' predicted presence and absence into binary patches, where each patch is composed of one or several adjacent pixels of the same type (e.g. presences). This biotic-centred approach contrasts with the classical application of landscape metrics where patches are often derived from land-cover maps (Uuemaa et al., 2013). Once patches of predicted presences and absences are identified, various landscape metrics can be used to characterise patch properties and their spatial structure, ultimately providing a better characterization of the internal range structure and how it will evolve in response to external pressures (e.g. climate change).

2 | MATERIALS AND METHODS

Our workflow, which combines landscape ecology metrics with species distribution model outputs is illustrated in Figure 1.

2.1 | Study area and species

The honeycomb worm *Sabellaria alveolata* is an intertidal ecosystem engineer, capable of building tubes from sand and shell fragments on low- to mid-shore, in semi-exposed and exposed locations. As a colonial species, the multitude of fused tubes form biogenic structures ranging from veneers and hummocks to large reefs (Wilson, 1971; Curd et al., 2019). Reef-forming *S. alveolata* has the potential to provide important coastal protection (Naylor & Viles, 2000) and biogenic habitat for a diverse range of other species (Dubois et al., 2002; Jones et al., 2018). *Sabellaria alveolata* has a discontinuous distribution ranging from southern Morocco to southwest Scotland (Lourenço et al., 2020), with many distribution breaks (Firth et al., 2021a) (Figure 2a).

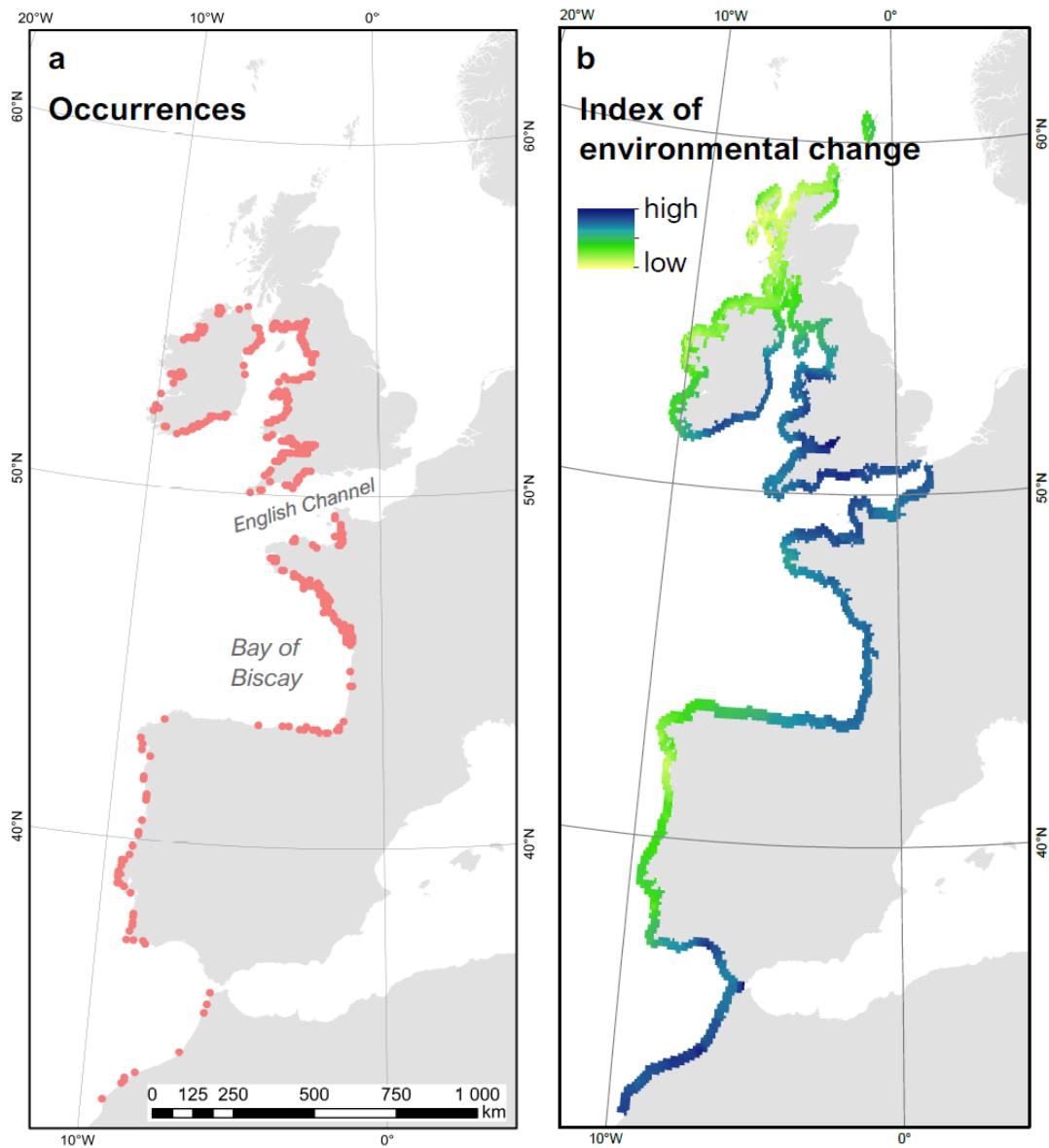


FIGURE 2. Species occurrence records and index of environmental change along the species distributional range. a, The 363 thinned occurrence records collated between 2000-2019 from multiple data sources highlight the broad but fragmented biogeographical range of *S. alveolata*. **b,** Index of change in local environmental conditions (Table S1) between current and future (RCP 4.5 in 2050) climatic layers. High values indicate the largest difference between current and future environmental conditions (for details regarding the index computation, see the Methods).

Our study was conducted across 29 degrees of latitude (from 32°N to 61°N) spanning a large gradient of climatic conditions (Figure S1). To the best of our knowledge *S. alveolata* is, and has always been, absent from the North Sea (Nunes et al., 2021). Although it has occasionally been cited as present in the North Sea (Richter, 1927), expert consensus is that these occurrences were *S. spinulosa* reefs (Reise, pers. comm.) (Figure S2). This distribution limit is thought to be due to the presence of a long-term hydrographic barrier to larval dispersal at the Cherbourg Peninsula in the English Channel (Salomon & Breton, 1993), and to competitive exclusion by *S. spinulosa* in the Greater North Sea. As both larval dispersal and biotic interactions cannot be accounted for by SDM, our study area does not extend to the North Sea. Since we only consider intertidal *S. alveolata* bioconstructions, our study area does not extend to the Mediterranean, where all *S. alveolata* records are subtidal owing to low amplitude tides.

2.1 | Occurrence records

An increasing number of SDM studies are based on presence data downloaded from the Global Biodiversity Information Facility (GBIF) (Alhajeri & Fourcade, 2019). Although these data have proved useful to model the distribution of some well-known species, records for *S. alveolata* are strongly affected by spatial sampling bias (Firth et al., 2021b) (Figure 2a). Here, we collated occurrence records from numerous sources, including field observations, research articles, citizen science observations, management reports and online databases (Curd et al., 2020). Presence records were considered between the years

2000-2019, a time span compatible with the temporal coverage of climatic layers classically used in SDM studies (e.g. Bio-ORACLE, Worldclim) (Assis et al., 2018; Hijmans et al., 2005; Tyberghein et al., 2012). Subtidal observations, and observations without geographic accuracy down to shore level, were excluded. Overall, 98 literature sources were included in the analysis, resulting in 14,960 occurrence records. Only 12.2% of these records were previously accessible via online databases (Curd et al., 2020). Occurrence records were spatially thinned so that only one record was retained per climatic-grid cell (Steen et al., 2021). This left us with 363 observations.

2.3 | Environmental variables

We retained only ‘scenopoetic’ variables (i.e. variables on which the species has no impact) as predictors (Hutchinson, 1978). We did not include available seabed substrate maps (although potentially relevant) because the best existing layer compilation (currently provided by EMODnet; <https://emodnet.ec.europa.eu/en>) was not deemed fit-for-purpose, due to low spatial accuracy in many areas and limited spatial coverage. All environmental predictors covered the full latitudinal distribution of *S. alveolata* and came at a spatial resolution of 0.083° decimal degrees. This corresponds to a distance of 9.3 km along the latitude axis and, along the longitude axis, while the distance along the longitude axis goes from 7.8km at the equatorward edge, to 4.5km at the poleward edge. Specifically, a set of 10 bioclimatic variables were chosen as climate-related candidate predictors (Table S1) including air temperature (min, max and mean) from WorldClim version 1.4 (Hijmans et al., 2005), sea-surface temperature (min, max and mean) and mean salinity from Bio-

ORACLE (Assis et al., 2018; Tyberghein et al., 2012), wave height (Bricheno & Wolf, 2018), wave fetch (i.e. the distance over which wind-driven waves can build given the orientation of the coastline, Burrows, 2020) and tidal current and surface amplitudes from the TPX08 ATLAS solution (www.tpxo.net) (Egbert & Erofeeva, 2002; Egbert et al., 2010). Present and future wave height was estimated by applying the WaveWatch IIITM spectral wave model at a regional scale (Atlantic Europe) (Tolman, 2009). Because wave fetch was estimated at a 100 m resolution, we re-projected and upscaled this raster (using average values) to match with the resolution of the other rasters (i.e. 0.083° degrees).

We checked for collinearity between variables using Pearson's correlation coefficients. For pairs with Pearson's $|r| > 0.7$, we retained the variable known to be the most ecologically relevant (Araújo et al., 2019). This process led us to select six predictors: maximum sea-surface temperature, average salinity, minimum air temperature, wave fetch, wave height and tidal amplitude (Figures S3-S7).

Future predictions for four of the six selected predictors were obtained for horizon 2050 under the Representative Concentration Pathway scenario RCP 4.5 (Meinshausen et al., 2011): salinity and sea surface temperature from Bio-ORACLE, air temperature from WorldClim and wave height from Bricheno & Wolf (2018). Tidal amplitude and wave fetch were assumed to stay constant in the future. To evaluate where, over the range, climate change might have the strongest effect on *S. alveolata* reefs, we calculated an index of environmental change. For this purpose, we first computed a climatic space using a principal component analysis (PCA) performed on the four standardised environmental variables that are predicted to change in the future (Figure S8). Then, we projected future

environmental values within the two-dimensional space defined by the two first PCA axes (explaining 82% of the variance). Hence, a given pixel has two positions in this space. The index was calculated as the Euclidean distance between present and future conditions for each pixel (Figure 2b) with greater distances indicating larger changes.

2.4 | Model building

Model building was performed in R (R Core Team, 2019) using the package ‘biomod2’ (Thuiller et al., 2009). Four fundamentally different algorithms were selected to build the SDMs: generalised linear models (McCullagh & Nelder, 1998), generalised additive models (Hastie & Tibshirani, 1986), random forests (Breiman, 2001), and boosted regression trees (Elith et al., 2008). The four algorithms have already proven useful in modelling benthic species distributions (Bučas et al., 2013) and were selected for their ability to model non-linear relationships while assuming different shapes for the response curves. These algorithms have their own set of strengths and weaknesses which can lead to contrasted predictions (de la Hoz et al., 2019). For instance, random forests generally display high predictive performance on the training dataset (Elith, 2006; Reiss et al., 2011) but are prone to overfitting which can yield inaccurate predictions when extrapolating to non-analog conditions (Wenger & Olden, 2012; Beaumont et al., 2016). Alternatively, GLMs often have a lower predictive accuracy on the training dataset but usually display higher transferability (Wenger & Olden, 2012; Heikkinen et al., 2012; Yates et al., 2018). Algorithms were fitted using the default settings of biomod2.

The four approaches require presence-absence data to be fitted. Since the absence records in our database had an uneven spatiotemporal spread (see Figure S1), we generated a random set of pseudo-absences over the study area. We generated the same number of pseudo-absences as available presences (i.e. 363) to give an equal weight to presences and absences in model predictions (Barbet-Massin et al., 2012). Models were then fitted on this presence/pseudo-absence dataset. To account for stochasticity regarding the selection of pseudo-absences, this procedure was repeated 10 times (i.e. ten pseudo-absence datasets were generated). Note that since we used pseudo-absences, the models predict a habitat suitability index ranging from 0 to 1 rather than a probability of presence (Guisan et al., 2017) (Figure S9).

2.5 | Model performance and ensemble predictions

Models were evaluated using a cross-validation approach based on repeated split-sampling (70% for calibration, 30% for evaluation) with 10 runs (Figure 1). For each run (and each pseudo-absence dataset), model performance was assessed using the true skill statistic (TSS) (Allouche et al., 2006) and the area under the ROC curve (AUC; Hanley and McNeil 1982). Both TSS (Sensitivity + Specificity - 1) and AUC are prevalence (i.e. the ratio of 'presence' to 'absence' in the dataset) independent. They provide information on the model's capacity to distinguish between presence and absence classes, with higher values pointing to better models (Lawson et al., 2014). Overall, a total of 400 models (4 algorithms

times 10 cross-validations times 10 pseudo-absence samplings) were fitted. The importance of the different predictors across datasets and algorithms was evaluated using the “variables_importance” function of biomod2.

We used an ensemble modelling approach to perform current and future predictions over the distribution range (Hao et al., 2020). Only models whose predictions on the test data had a TSS ≥ 0.5 were retained for this procedure (99 GAM + 89 GLM + 100 RF + 99 BRT). Current and future predictions from the 387 contributing models were combined using a weighted average based on TSS scores (i.e. higher influence of models or datasets with higher TSS). Present and future predictive ensemble maps were reclassified into binary presence-absence surfaces using the threshold that maximises TSS evaluation scores (i.e. maxTSS; Guisan et al., 2017).

2.6 | Measuring broad-scale external range changes between periods

Binary predictions are classically used to estimate how species ranges will be affected in the future (Yalcin & Leroux, 2017). While the main object of inference focuses on range size (Gaston, 1996), additional metrics can be found in the literature (e.g. the proportion of pixels lost or gained) (Thuiller, 2004). When considering a broad latitudinal gradient, a more accurate estimation of changes in range size can be obtained by giving an equal area to all pixels (Sillero & Barbosa, 2021). Here, we re-projected the predicted rasters (both for presence-absence and habitat suitability) with the ETRS89 Lambert Azimuthal Equal Area Coordinate Reference System (ETRS-LAEA), with the latitude and the longitude of origin adjusted to 44.3°N, -3.2°E, giving each pixel an area of 25 km² (5 km x 5 km). From

the presence-absence rasters, we used the BIOMOD_RangeSize function to estimate the proportion and relative number of pixels lost, gained and stable. We also quantified range shifts, another measure frequently used to estimate the effect of climate change on species distribution (e.g. Lenoir et al., 2020). To measure this, we first characterised ranges in both periods considering the centre (median latitudinal value where the species was predicted to be present), the upper (97.5% percentile) and the lower (2.5% percentile) limits of the range. We then quantified range shifts for all three attributes as the difference between future and current values.

2.7 | Measuring fine-scale internal range changes between periods

In addition to broad-scale range metrics that describe external range changes, we used landscape metrics to better characterise the fine-scale internal structure of the species range (in both current and future climatic conditions) and provide additional insights regarding how this structure will be affected in the future. Landscape ecologists often conceptualise the landscape as a mosaic of discrete, ecologically homogeneous, patches embedded within a background matrix of inhabitable areas (Turner et al. 2005, Lausch et al. 2015). Patches are the basic statistical unit under this approach, and are defined as one isolated, or several adjacent, pixels of the same class (e.g. crops) that differ from their surroundings (e.g. forests). Each patch has its own individual characteristics (e.g. shape, size, distance to nearest neighbour; Hesselbarth et al. 2019), while the landscape pattern emerges from the spatial composition and configuration of patches from different classes (Turner et al. 2005, Lausch et al. 2015). Pixels belonging to each patch can be monitored over time so that

pixels transitioning from one class to another in response to external pressures (e.g. climate change) can be translated into patch dynamics. Thus, presence pixels switching to absence pixels within a presence patch lead to patch fragmentation. A suite of landscape metrics describing changes in patch properties (e.g. area, Euclidean distance to the nearest neighbour), and their spatial configuration (e.g. patch aggregation) can also be used to describe changes at various spatial scales. For instance, an increased distance to the nearest neighbour coupled with a decrease in patch aggregation for presence patches is indicative of population fragmentation.

Here, we propose to use landscape metrics on predicted binary (presence and absence) maps obtained from SDMs to simplify, often complex, spatial predictions into a mosaic of discrete patches of predicted presences and absences under both current and future environmental conditions. Landscape metrics can then be used to study presence and absence patch properties and how their spatial arrangement is predicted to change in the future, ultimately providing a better characterization of range changes.

Landscape metric analyses were performed using the R package ‘landscapemetrics’ (Hesselbarth et al., 2019). This package contains many functions to describe various patch properties (e.g. area, distance to nearest neighbour of the same class). These properties can be aggregated at different spatial scales (e.g. mean patch area at the range scale) and studied over time. Note that the package also provides functions to compute diversity metrics at the landscape scale (i.e. range scale in our case), however since our usage is constrained to binary outputs, most of these functions were not relevant for the purposes of this study. Here, we focused on the patch area for each class, the Euclidean distance to the nearest

neighbouring patch of the same class, and the predicted habitat suitability of pixels within patches (a metric that uses an additional level of information derived from SDMs). The latter metric relies on the fact that each pixel contains additional quantitative information (i.e. the habitat suitability values that were used for thresholding which is a necessary step to identify patches) that can be used to better characterise patch properties and their spatial arrangement. Here, we used this information to run a patch-based linear regression to investigate whether average changes in patch suitability (i.e. the average difference between future and current suitability for all pixels within the patch) followed a latitudinal gradient, a classical biogeographical pattern where species are moving poleward to track suitable climatic conditions (Mieszkowska & Sugden, 2016).

3 | RESULTS

3.1 | Model performance and variable importance

Ensemble model predictions of present distribution performed well (AUC = 0.91 ± 0.03 ; TSS = 0.67 ± 0.05 - Table S2 and Figure S10) in characterising the large-scale, yet fragmented, latitudinal range of *S. alveolata* (specificity score 0.78 ± 0.06 ; Figure 3a). Predicted areas of absence (e.g. southern French Atlantic coast) also matched well with current observed absence data (Figures 2a and 3a, Figure S1). Fetch was the most important variable (explaining 35% of variance), suggesting that coastal exposure to wind-wave action, a local to regional scale feature, is a primary determinant of habitat suitability (Table S3 and Figure S7). Dynamic temperature variables and ocean variables had less influence

on model predictions but were still critical to characterise broad-scale geographic range. In fact, sea surface and air temperature were the second and fourth most important variables, respectively, while salinity was the third most important variable (Table S3). See Figure S11 for variable response curves.

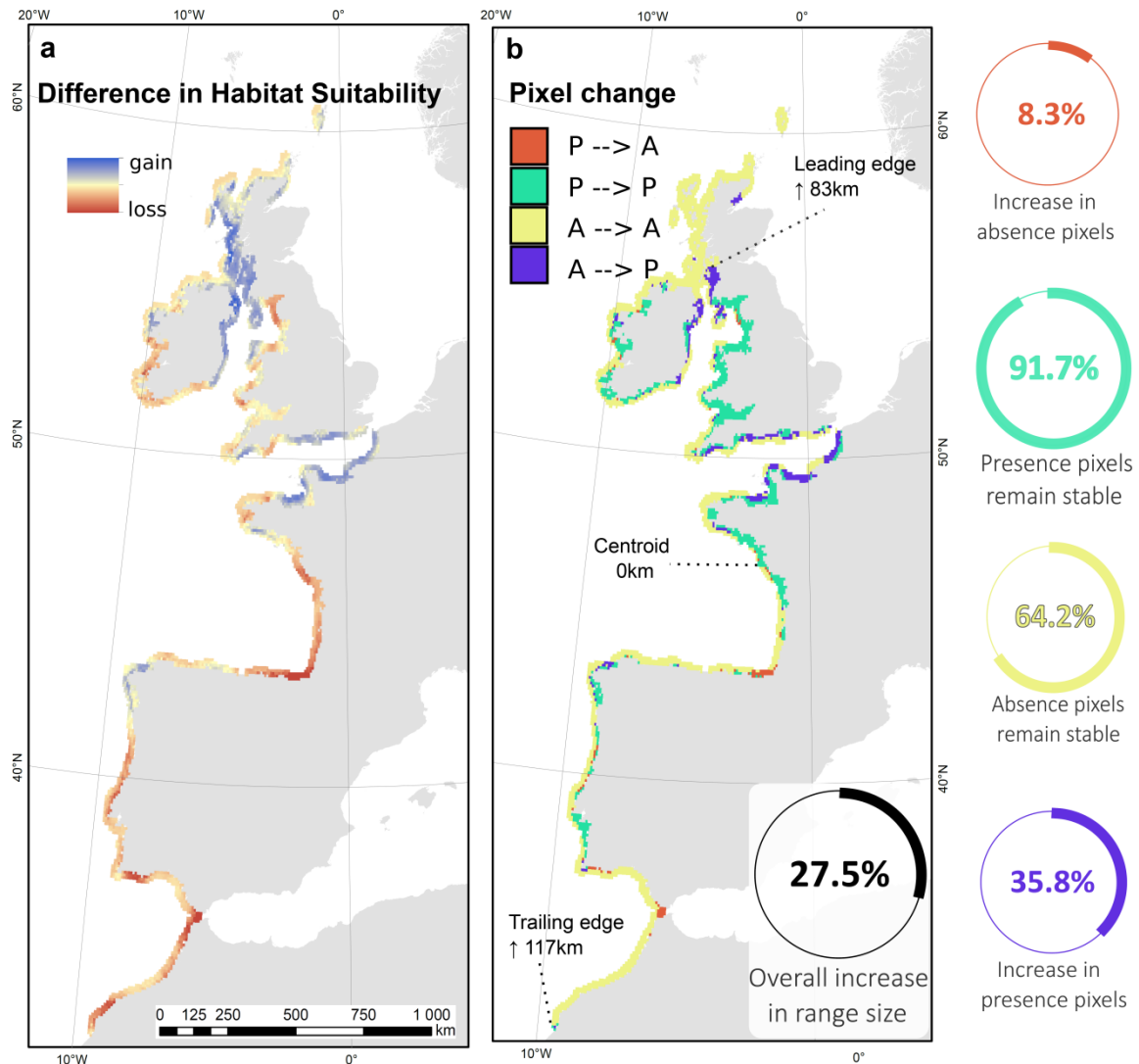


FIGURE 3 Predicted difference in habitat suitability and presence-absence patterns between current and future (RCP 4.5 2050) climatic conditions. a, Difference in habitat suitability between present and future, with blue colours indicating a future increase in habitat suitability, and red colours indicating a future loss in habitat suitability (yellow colours represent an absence of change). **b,** Change in presence/absence predictions between the present and future. Orange pixels (P → A) = shift from current presence to future absence; green pixels (P → P) = stable presence pixels; yellow pixels (A → A) = stable absence pixels; violet pixels (A → P) = shift from current absence to future presence. Predictions were binarised using a max TSS threshold of 0.53. Leading edge = 95% quantile of the latitudinal range, Trailing edge = 5% quantile of the latitudinal range, centroid = range centre/optimum median.

3.2 | Broad-scale range changes

The ensemble model predicts a 27.5% increase in range size (Figure 3b), with future gains predicted to mostly occur around the Irish Sea, on both sides of the English Channel and along the coast of Galicia (Spain) (Figure 3a). Overall, we found large spatial heterogeneity in the proportion of pixels predicted to become suitable (35.8%), unsuitable (8.3%) and stable (91.7% of absence pixels and 64.2% of presence pixels) in the future (Figure 3b). This heterogeneity leads to an overall contraction of the latitudinal range owing to a greater retraction of the trailing edge relative to the extension of the leading edge (117 km vs. 83 km respectively; Table S4, Figure 3b). Although other local changes are visible, they are not captured by broad-scale range metrics.

3.3 | Within-range changes

The application of landscape metrics enabled us to identify 90 patches (both presences and absences) in the current time period, and 92 patches in the future. While mean habitat suitability per patch increased with latitude ($P < 0.001$; $R^2 = 0.41$), 59% of the variability in patch suitability remained unexplained, highlighting departures from expectations (i.e. a global poleward shift).

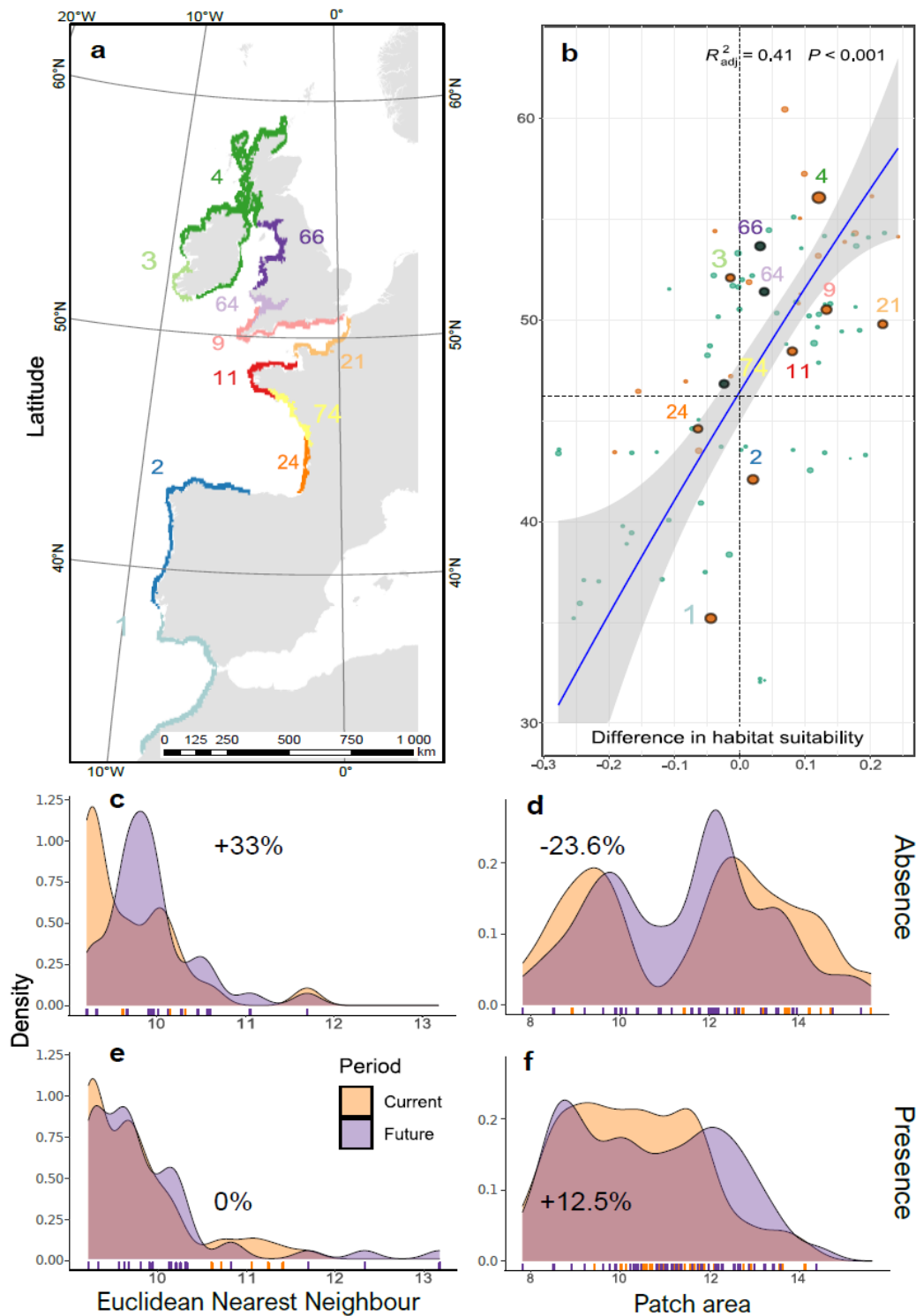


FIGURE 4 Overview of presence-absence patches and changes between time periods for selected patch and landscape metrics. **a**, Map of 2000-2019 presence/absence

patches. Numbered regions map to their equivalent 'bubbles' in (b). **b**, Change in average patch habitat suitability between current (2000-2019) and future (RCP 4.5 2040-2049) as a function of latitude. Current presence patches are displayed in green whereas current absence patches are in orange. Bubble size indicates patch area. The horizontal dashed line points to the latitude at which the predicted difference in habitat suitability switches from negative to positive. Latitude was treated as the independent variable but the axes were flipped for presentation purposes. Density plots highlighting changes in patch level Euclidean nearest neighbour (ENN) distance for both absence (**c**) and presence patches (**e**), whilst (**d**) and (**f**) show the change in patch area for absences and presences respectively. For each density plot, the proportional change between future and current median values, relative to the current period, are highlighted.

Despite an overall stability in the total number of patches between current and future conditions, presence patches are predicted to decrease from 65 to 56 (-14%), while absence patches are predicted to increase from 25 to 36 (+31%) (Figures S12 and S13). This does not however mean that absences are more prevalent in the future, owing to a global increase in the size of presence patches (+12.5%) combined with a decrease in the size of absence patches (-23.6%) (Figures 4d and 4f). The average distance (Euclidean nearest neighbour; Figures 4c and 4e) between patches is predicted to increase in the future for absences (+33%) but to remain stable for presences. The geographic distribution of presence and absence patches is also predicted to change. For instance, presence patches are predicted to coalesce poleward, with the formation of a large presence patch along the west coast of Britain and Ireland, while most equatorward patches are predicted to fragment (Figures 3b and 4e).

Future predictions show that patches can behave in one of four ways. Either presence and absence patches can expand, or patches of presence can appear in areas of absence and vice-versa. An example of each specific case is presented in Figure 5, with associated local-scale landscape metrics. Note that these metrics can be obtained within any section of the range. For instance, when considering the southwest coast of England, we predict that five presence patches will merge into one larger presence patch in the future owing to multiple absence pixels predicted to become suitable (Figure 5b). Focusing on this region, this change leads to a 400% increase in the Largest Patch Index (LPI), the largest presence patch dominating 20% of this regional landscape under current conditions, and 100% under future conditions. In the current range centre (north Bay of Biscay), we predict a localised extirpation in the centre of a large presence patch (Figure 5c), increasing edge pixels between presence and absence patches and thus decreasing the percent of core area (-6%). In northern Spain and the southern Bay of Biscay, we predict the disappearance of small presence patches within a large absence area (Figure 5d), increasing the total area of absences by nearly 18% within this region (total class area metric). Finally, along the northwest Iberian Peninsula, numerous small areas of suitable habitat are predicted to appear in a currently large absence patch (Figure 5e), leading to a 1% decrease in aggregation index (from 86% under current conditions to 85% in the future).

4 | DISCUSSION

In this study, we aimed to illustrate how and to what extent broad-scale metrics, that mostly describe external range changes, can overlook the more nuanced internal range changes

that can take place under climate change. For this purpose, we focused on changes predicted under current and future (2000-2019 vs. 2040-2049) environmental conditions for a species with a naturally discontinuous distribution: *Sabellaria alveolata*. We then investigated how broad-scale range metrics can be complemented by landscape metrics to better characterise the effect climate change can have on species geographic ranges. Overall, we found that broad-scale range metrics alone would have led to the conclusion that the study species is a climate change winner. Within-range changes provided additional insights by revealing that the range will become increasingly fragmented in its equatorward half in the future, with potential implications for local declines and extirpations. As *S. alveolata* underpins myriad ecosystem functions (Dubois et al., 2002; Jones et al., 2018) changes in its distribution (i.e. presence-absence, hence occupancy of suitable habitats) and abundance are likely to have adverse cascading effects on ecosystem services (Wetthey et al., 2011).

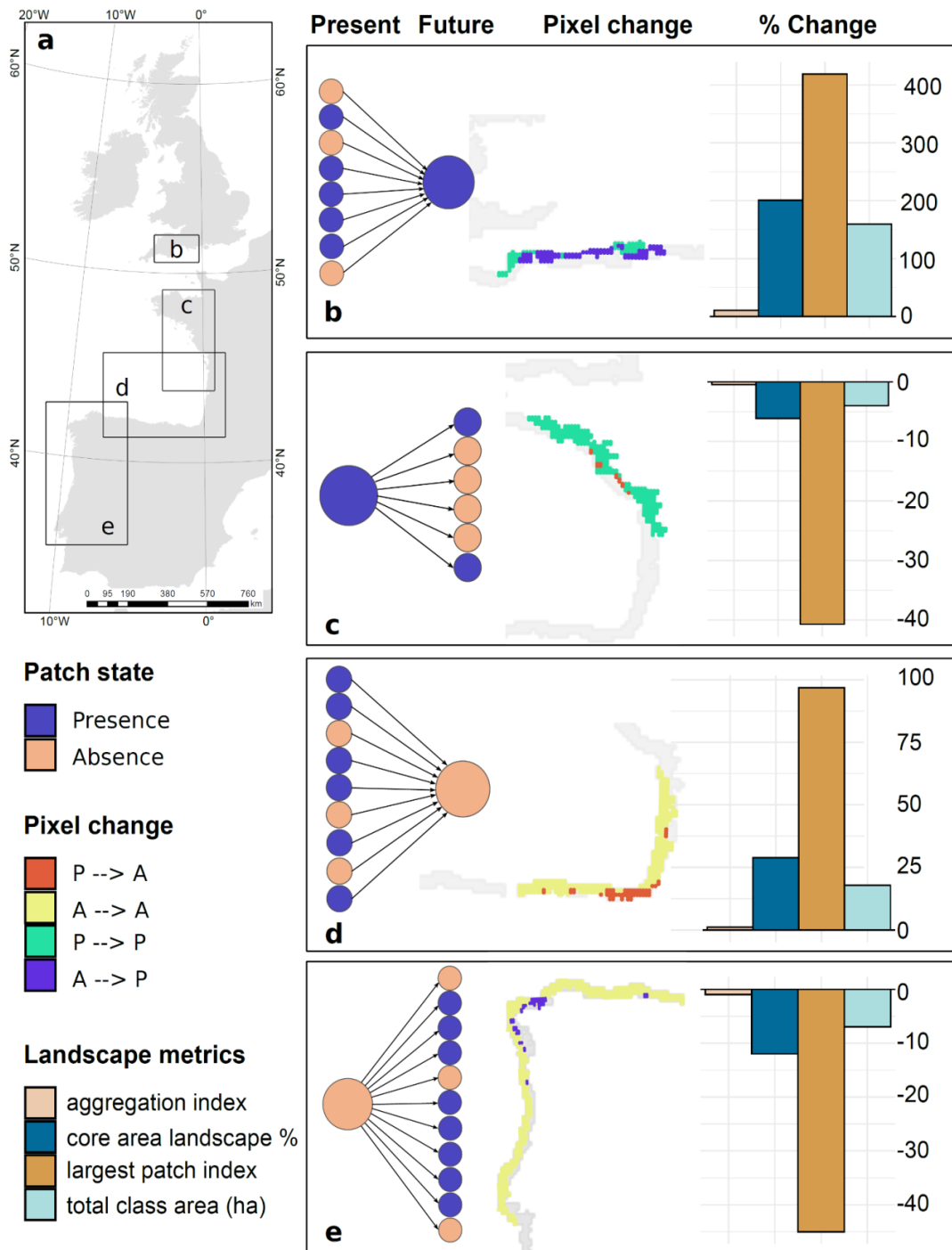


FIGURE 5 Examples of internal range change. The four types of patch transitions, with barplots of associated landscape metrics. **a**, Location of all four examples. **b**, Expansion of presence patches **c**, Absence patches appearing in a larger presence patch. **d**, Expansion of absence patches. **e**, Presence patches appearing in a large absence patch. The barplots

represent relative changes in different landscape metrics relative to baseline metrics calculated under current environmental conditions: negative values indicate a decrease of the metric in the future and positive values indicate the opposite. In all four examples, the coloured pixels define the landscape on which the metrics are computed. The largest patch index is the percentage of the landscape covered by the largest patch. The aggregation index describes the extent to which patches of the same class are aggregated. The total class area is the sum of the area of all patches of the same class. Finally, the core area landscape is the average of the percentage of core area (i.e. patch area without edge pixels) in relation to total patch area.

Despite the recognised ecological and economic value of ecosystem engineers in terms of biodiversity and ecosystem functioning (Ellison et al., 2005; Lemasson et al., 2017), to our knowledge, only a handful of studies have simultaneously considered terrestrial and marine environmental conditions to which coastal ecosystems are exposed (e.g. Lima et al., 2013; Boo et al., 2019); so far only one study has focused on an ecosystem engineer (Faroni-Perez, 2017). Our results confirm that both air and seawater temperatures are ultimate drivers of changes in sabellarid distribution (Faroni-Perez, 2017; Firth et al., 2015; Firth et al., 2021a), thus confirming its status as an indicator of climate change in Britain and Ireland (Mieszkowska et al., 2006). However, patterns of change are predicted to differ between biogeographic regions owing to the effect of other local factors (Firth et al., 2021a). For instance, our study suggests that the effect of temperature can be overridden by local and regional factors determined by coastline orientation, especially due to fetch.

While the overall increase of habitat suitability predicted by SDM would categorise *S. alveolata* as a climate change ‘winner’ (Somero, 2010), a closer look at SDM predictions highlights a more nuanced situation owing to a complex interplay of various factors. First, *S. alveolata* is predicted to reach the very north of Britain and Ireland by 2050, but in the longer-term future (e.g. the 2090s), its poleward expansion will be limited by the lack of continuous or connected landmass, as is the case for a number of other coastal species in northwest Europe (Philippart et al., 2011). Some longer-term colonisation of the outer islands of the British Isles (Hebrides, Orkney, Shetland) might be possible, but may be dispersal-limited. This suggests that proximate factors such as habitat availability (supply of sand for tube building adjacent to hard substrata for adhesion) and dispersal ability may override the ultimate drive of climate change (Harley et al., 2006). Second, the predicted shrink of the latitudinal range (Figure 3b) indicates that the distribution will be mostly clustered in poleward regions but increasingly fragmented in equatorward regions (Figure 4), a process that could disrupt connectivity networks between isolated populations. This is particularly concerning in the equatorward part of *S. alveolata*'s range given that it is currently located within the Canary Eastern Boundary Upwelling System, where a rapid warming at its trailing edge is occurring ($0.60^{\circ}\text{C decade}^{-1}$ off Mauritania), leading to speculation that an upwelling shutdown or geographic shift has already begun (Seabra et al., 2019). This pattern matches well with previous findings showing that leading (poleward) and trailing (equatorward) edges respond differently to climate change (Poloczanska et al., 2013). At the leading edge, larger occurrence patches could strengthen regional connectivity, which could favour inter-seeding between distant populations and enhance species regional resilience to local perturbations or extreme climatic events. In

contrast, at the trailing edge, increased distance between presence patches could lead to a loss of genetic diversity in threatened former core areas of the range (Nicastro et al., 2013). Thus, while some presence patches located at the trailing edge are predicted to increase in habitat suitability (e.g. the patch located close to Morocco is predicted to increase from 0.53 to 0.57), their increasing isolation could actually lead to an increased extirpation risk. If this happens, the trailing edge would shift to southern Spain (Gulf of Cadiz), leading to a further range contraction of 500 km. Third, while trailing and leading edges are clearly identified by SDM predictions, our model further predicts a strong decrease in habitat suitability in the central part of the range along the French Atlantic coast (Figure 3b), a critical region for this species where it forms extensive reefs (surface cover (100s ha) and height (>1m)) (Curd et al., 2020). A decrease in habitat suitability in this region could lead to a break in connectivity between the equatorward and poleward parts of the range, should the gap between the two regions exceed the dispersal abilities of the species (Wort et al., 2019).

The three preceding points suggest that *S. alveolata* may not, at a global scale, be a climate change winner. Up until now, such detailed changes required expert knowledge and a deep understanding of the ecology of the focal species, which are very difficult to attain particularly in multi-species studies. We propose to use additional landscape metrics, transposable from one species to another, to adequately and generically describe the complex changes taking place within species ranges. While not replacing the critical value of expert-based interpretations, this approach could help pinpoint more complex changes than the ones reported with broad-scale range metrics. Overall, our results indicate that

landscape metrics, and particularly the Euclidean nearest neighbour distance between patches of the same class, are valuable to identify vulnerable and isolated patches, and can help inform regional management strategies (e.g. promoting ecological connectivity among populations). For instance, the identification of isolated patches could be used to locate further work on larval dispersal and recruitment, along with genetic diversity studies to help understand how separate patches of presences are interconnected and therefore whether they are part of a metapopulation functioning. Such studies are of particular interest given the role of isolated populations in evolutionary processes (see Supplementary Text).

More generally, several landscape metrics could be used to describe the extent to which various patch properties (e.g. area, aggregation patterns) are predicted to change in the future. Similarly to global change metrics classically reported in SDMs studies, we encourage future studies to report such internal range metrics to better predict climate change effects on species ranges. Interestingly, these metrics can be calculated at different user-defined resolutions, giving the possibility to study changes taking place at different spatial scales (e.g. regional, global, Chase et al. 2018). The issue of scale is at the core of landscape ecology (Turner et al. 2005) and previous studies have reviewed its effects on landscape metrics (e.g. Newman et al. 2019). Applying landscape metrics to SDM outputs adds another layer of complexity, since the accuracy of SDM predictions also varies depending on the spatial resolution and the scale considered (e.g. Chauvier et al. 2022). Here, we defined a patch as a minimum of one isolated pixel because of the broad-scale nature of the study. For finer-scale studies, a given number of pixels per patch could be set

as a threshold. The latter could be based on ecological knowledge (e.g. dispersal distance), or by setting arbitrary thresholds and subsequently conducting a sensitivity analysis. Beyond landscape metrics, the fact that patches and associated pixels are characterised by unique identifiers further makes it possible to study in more detail (e.g. regional or species-centred studies) how patches of presences and absences are predicted to fragment or coalesce in the future. For instance, despite the stable number of patches predicted in the future, multiple colonisation and extinction events are predicted throughout the range, leading to current patches (of presences or absences) either splitting into several patches or merging with existing patches (Figure 5, Figures S12 and S13, Table S5). The predicted merging of presence patches in southwest England suggests that greater dispersion among existing presence patches in this area could either foster a range expansion, or resilience increase. In the current range centre (north Bay of Biscay), we predict a localised extirpation in the centre of a large presence patch, leading to a future gap between two presence patches. Similarly, between trailing edge populations (northern Spain) and populations from the Bay of Biscay, we predict local extirpations of a potential key stepping-stone population within a large absence area, with potential implications for connectivity. Finally, the predicted appearance of several small patches of suitable habitat within a currently large absence patch along the northwest Iberian Peninsula reinforces the importance of conservation efforts covering small habitat areas, as integrating key fragments in coastal management could benefit long-term species persistence. Beyond population connectivity, the predicted changes in spatial configuration may alter ecosystem functioning and dynamics. Spatial configurations are intrinsically linked with regime stability or shifts (Kefi et al., 2014). Landscape metrics can provide information on internal

range changes which can act as early warning signals of impending regime shifts (Nijp et al., 2019). Relatively simple statistical landscape metrics are therefore critical for conservation, and could perhaps even fuel other types of analysis aiming to understand spatial early warning signals as ecosystems approach a tipping point (Génin et al., 2018).

The extirpation of ecosystem engineers and the related cascading ecosystem effects are considered principal drivers of regime shifts in both marine and terrestrial realms (Estes et al., 2018; Wright, 2009). There are, however, also consequences when the range of an ecosystem engineer shifts due to climate change, enabling colonisation of individuals and persistence of populations into new areas. The potential gain of an extensive area of suitable habitat, in Britain and Ireland, could alter community structure and ecosystem processes, with ensuing positive and negative impacts (Bulleri et al., 2018; Wallingford et al., 2020). It is also possible that species inhabiting *S. alveolata* reefs will exhibit range extensions by using the new areas of reef occurrence as “stepping stones”, with climate change facilitating the dispersion of the associated biota into new territories (Dubois et al., 2002; Faroni-Perez 2017), aided by proliferating sea defences as a societal adaptational response to rising and stormier seas driven by climate change (Bugnot et al., 2021; Firth et al., 2015). As a biogenic habitat forming species, it could also promote the diversity and resilience of benthic fauna by providing improved environmental conditions in the face of climate change through facilitation or habitat cascades (Bulleri et al., 2018; Gribben et al., 2019). The duality of effects upon recipient communities underscores the importance of considering the ecological impacts of species exhibiting range-shifts, in terms of both the benefits and potential costs to associated biodiversity and ecosystem functioning and

service provision (Wallingford et al., 2020). Despite fundamental differences between introduced non-native and naturally range-shifting species, they can impact communities via analogous mechanisms (Wallingford et al., 2020). Landscape metrics could therefore also be useful for invasion risk assessments at a spatial scale relevant to regional and local-scale management decisions, e.g. Marine Protected Areas.

Several studies have used landscape metrics as covariates in SDMs to improve model predictions (Hasui et al., 2017; Ortner & Wallentin 2020). The novelty in our approach lies in the application of landscape metrics to binary predictions obtained from SDMs (or any spatial model e.g. joint-SDMs or mechanistic models) in order to identify patches of absences and presences. This framework makes it possible to study the internal range structure of species and better characterise the evolution of species ranges in response to e.g. climate change, provided that predictions are robust (i.e. our approach does not circumvent the flaws inherent to spatial models and does not improve their accuracy). For instance, selected landscape metrics can either reinforce or hinder the conclusions drawn from global change metrics. Here, we have shown a global increase in the range area (+27%) but further found that this global increase was mostly due to one presence patch largely increasing in the northern part of the range (coalescing with other presence patches) while most other presence patches were collapsing. While providing some avenues regarding how changes in landscape metrics could be interpreted when applied to SDMs outputs, the choice of landscape metrics and their interpretation will ultimately depend on the study system and question. Here we focused on the effect of climate change; however SDMs have been used for many other purposes (Bellard et al. 2012) where the use of

landscape metrics would still be valuable. For instance, patch size and nearest neighbour metrics can be used jointly to identify patches that will become increasingly isolated in the future and for which conservation actions may be needed.

5 | CONCLUSIONS

As Earth's climate rapidly changes, individuals of a species must move, acclimate, adapt, or die. Range shifts are therefore key to species persistence (Muir et al., 2020). Beyond range size and boundaries, internal range structure metrics are needed to adequately describe species' ranges and more accurately quantify how they will be affected in the future (Csergő et al., 2020), particularly for species with discontinuous distributions. Analysing which landscape-level processes scale up to structure biogeographic ranges of species has however remained largely unexplored. Recent work however provides evidence that population and species level responses to habitat change at the landscape scale are modulated by factors and processes occurring at macroecological scales, such as historical disturbance rates, distance to geographic range edges, and climatic suitability (Banks-Leite et al., 2022). Our results suggest that these landscape-scale processes may be key to understanding and predicting internal range reconfiguration in changing environments. Specifically, we showed that broad-scale SDM combining terrestrial and marine predictors, coupled with a selection of global and regional landscape metrics, can be used to more accurately describe the changes a widely distributed intertidal species will face. Fragmentation of occupied area or suitable habitat has already been identified as a

better predictor of extinction risk than range size (Crooks et al., 2017), and we propose that metrics characterising different aspects of species range structure, such as the distance between patches of suitable habitat, may be useful to meet conservation targets.

Conservation efforts should be refocused to search for critical internal range structure thresholds, especially those acting as proximate factors. Environmental management often focuses on single sites and populations, which crucially do not consider the wider context. Landscape metrics applied to SDM outputs are a robust, non-data-intensive method that can aid environmental managers with broad-scale spatial planning under climate change.

AUTHOR CONTRIBUTIONS

A.C., L.B.F. and S.F.D. conceived this research. M.C., M.V., A.B. and M.P.M. analysed species distribution data and developed the use of landscape metrics in combination with SDM outputs to better characterize changes in species internal range structure. L.M.B., M.T.B and J.A.M.G. provided the oceanographic data for wave, fetch and tide respectively. A.C., L.E.B., C.C., A.J.D., S.F.D., L.B.F., S.J.H., F.P.L., C.M., N.M. and R.S. contributed towards the species distribution data. A.C. wrote the first draft. A.C., M.C., L.B.F., S.F.D., A.B., M.V. and M.M. contributed equally to discussion of ideas and analyses. M.C., A.J.D., L.B.F. and S.J.H. provided substantial inputs on drafts and revisions of the paper. All authors commented on the manuscript.

ACKNOWLEDGEMENTS

We thank the many field assistants and citizen scientists who have gathered data on *Sabellaria alveolata* along Europe's coastline over many years. AC was funded by a PhD grant from Ifremer. This study was financially supported by the Total Foundation [Grant No. 1512 215 588/F, 2015]. The wave modelling was supported by the European Union's Seventh Programme for Research, Technological Development, and Demonstration under grant agreement FP7-ENV-2013-Two-Stage-603396-RISES-AM- and the ARCHER UK National Supercomputing Service <http://www.archer.ac.uk>.

CONFLICT OF INTEREST

The authors declare that they have no competing interests.

DATA AVAILABILITY STATEMENT

The *S. alveolata* records dataset is archived as a .csv file in the SEANOE data repository (<https://doi.org/10.17882/72164>). All sources of environmental predictors used for modelling are freely available and referenced in Table S1. The code that supports the findings of this study is available from https://github.com/Mathieu-Chevalier/SDM_landscape_metrics

REFERENCES

Alhajeri, B. H., & Fourcade, Y. (2019). High correlation between species-level environmental data estimates extracted from IUCN expert range maps and from GBIF occurrence data. *Journal of Biogeography*, 46(7), 1329–1341.

- Allouche, O., Tsoar, A., & Kadmon, R. (2006). Assessing the accuracy of species distribution models: Prevalence, kappa and the true skill statistic (TSS): Assessing the accuracy of distribution models. *Journal of Applied Ecology*, 43(6), 1223–1232. <https://doi.org/10.1111/j.1365-2664.2006.01214.x>
- Araújo, M. B., Anderson, R. P., Márcia Barbosa, A., Beale, C. M., Dormann, C. F., Early, R., Garcia, R. A., Guisan, A., Maiorano, L., Naimi, B., O’Hara, R. B., Zimmermann, N. E., & Rahbek, C. (2019). Standards for distribution models in biodiversity assessments. *Science Advances*, 5(1), eaat4858. <https://doi.org/10.1126/sciadv.aat4858>
- Assis, J., Tyberghein, L., Bosch, S., Verbruggen, H., Serrão, E. A., & De Clerck, O. (2018). Bio-ORACLE v2.0: Extending marine data layers for bioclimatic modelling. *Global Ecology and Biogeography*, 27(3), 277–284. <https://doi.org/10.1111/geb.12693>
- Banks-Leite, C., Betts, M. G., Ewers, R. M., Orme, C. D. L., & Pigot, A. L. (2022). The macroecology of landscape ecology. *Trends in Ecology & Evolution*, S0169534722000052. <https://doi.org/10.1016/j.tree.2022.01.005>
- Barbet-Massin, M., Jiguet, F., Albert, C. H., & Thuiller, W. (2012). Selecting pseudo-absences for species distribution models: How, where and how many?: How to use pseudo-absences in niche modelling? *Methods in Ecology and Evolution*, 3(2), 327–338. <https://doi.org/10.1111/j.2041-210X.2011.00172.x>
- Barbier, E. B., Hacker, S. D., Kennedy, C., Koch, E. W., Stier, A. C., & Silliman, B. R. (2011). The value of estuarine and coastal ecosystem services. *Ecological Monographs*, 81(2), 169–193.

- Beaumont, L. J., Graham, E., Duursma, D. E., Wilson, P. D., Cabrelli, A., Baumgartner, J. B., Hallgren, W., Esperón-Rodríguez, M., Nipperess, D. A., & Warren, D. L. (2016). Which species distribution models are more (or less) likely to project broad-scale, climate-induced shifts in species ranges? *Ecological Modelling*, 342, 135–146.
- Boo, G. H., Qiu, Y., Kim, J. Y., Ang, P. O., Bosch, S., De Clerck, O., He, P., Higa, A., Huang, B., Kogame, K., Liu, S., Nguyen, T., Suda, S., Terada, R., Miller, K. A., & Boo, S. M. (2019). Contrasting patterns of genetic structure and phylogeography in the marine agarophytes *Gelidiophycus divaricatus* and *G. Freshwateri* (Gelidiales, Rhodophyta) from East Asia ¹. *Journal of Phycology*, jpy.12910. <https://doi.org/10.1111/jpy.12910>
- Breiman, L. (2001). Random forests. *Machine Learning*, 45(1), 5–32.
- Bricheno, L. M., & Wolf, J. (2018). Future Wave Conditions of Europe, in Response to High-End Climate Change Scenarios. *Journal of Geophysical Research: Oceans*, 123(12), 8762–8791. <https://doi.org/10.1029/2018JC013866>
- Bučas, M., Bergström, U., Downie, A.-L., Sundblad, G., Gullström, M., von Numers, M., Šiaulyš, A., & Lindegarth, M. (2013). Empirical modelling of benthic species distribution, abundance, and diversity in the Baltic Sea: Evaluating the scope for predictive mapping using different modelling approaches. *ICES Journal of Marine Science*, 70(6), 1233–1243. <https://doi.org/10.1093/icesjms/fst036>
- Bugnot, A. B., Mayer-Pinto, M., Airoidi, L., Heery, E. C., Johnston, E. L., Critchley, L. P., Strain, E. M. A., Morris, R. L., Loke, L. H. L., Bishop, M. J., Sheehan, E. V., Coleman, R. A., & Dafforn, K. A. (2021). Current and projected global extent of

marine built structures. *Nature Sustainability*, 4(1), 33–41.

<https://doi.org/10.1038/s41893-020-00595-1>

Bulleri, F., Eriksson, B. K., Queirós, A., Airoidi, L., Arenas, F., Arvanitidis, C., Bouma, T. J., Crowe, T. P., Davoult, D., Guizien, K., Iveša, L., Jenkins, S. R., Michalet, R., Olabarria, C., Procaccini, G., Serrão, E. A., Wahl, M., & Benedetti-Cecchi, L. (2018). Harnessing positive species interactions as a tool against climate-driven loss of coastal biodiversity. *PLOS Biology*, 16(9), e2006852.

<https://doi.org/10.1371/journal.pbio.2006852>

Burrows, M. T., Hawkins, S. J., Moore, J. J., Adams, L., Sugden, H., Firth, L., & Mieszkowska, N. (2020). Global-scale species distributions predict temperature-related changes in species composition of rocky shore communities in Britain.

Global Change Biology, gcb.14968. <https://doi.org/10.1111/gcb.14968>

Burrows, M. (2020). *Wave fetch GIS layers for Europe at 100m scale* (p. 904169794

Bytes) [Data set]. figshare. <https://doi.org/10.6084/M9.FIGSHARE.8668127>

Chase, J. M., McGill, B. J., McGlinn, D. J., May, F., Blowes, S. A., Xiao, X., Knight, T. M., Purschke, O., & Gotelli, N. J. (2018). Embracing scale-dependence to achieve a deeper understanding of biodiversity and its change across communities. *Ecology Letters*, 21(11), 1737–1751.

<https://doi.org/10.1111/ele.13151>

Chauvier, Y., Descombes, P., Guéguen, M., Boulangeat, L., Thuiller, W., &

Zimmermann, N. E. (2022). Resolution in species distribution models shapes spatial patterns of plant multifaceted diversity. *Ecography*.

<https://doi.org/10.1111/ecog.05973>

- Crooks, K. R., Burdett, C. L., Theobald, D. M., King, S. R., Di Marco, M., Rondinini, C., & Boitani, L. (2017). Quantification of habitat fragmentation reveals extinction risk in terrestrial mammals. *Proceedings of the National Academy of Sciences*, 114(29), 7635–7640.
- Csergő, A. M., Broennimann, O., Guisan, A., & Buckley, Y. M. (2020). Beyond range size: Drivers of species' geographic range structure in European plants. *BioRxiv*, 2020.02.08.939819. <https://doi.org/10.1101/2020.02.08.939819>
- Curd, A., Pernet, F., Corporeau, C., Delisle, L., Firth, L. B., Nunes, F. L. D., & Dubois, S. F. (2019). Connecting organic to mineral: How the physiological state of an ecosystem-engineer is linked to its habitat structure. *Ecological Indicators*, 98, 49–60. <https://doi.org/10.1016/j.ecolind.2018.10.044>
- Curd, A., Cordier, C., Firth, L. B., Bush, L., Gruet, Y., Le Mao, P., Blaze, J. A., Board, C., Bordeyne, F., Burrows, M. T., Cunningham, P. N., Davies, A. J., Desroy, N., Edwards, H., Harris, D. R., Hawkins, S. J., Kerckhof, F., Lima, F. P., McGrath, D., ... Dubois, S. (2020). *A broad-scale long-term dataset of Sabellaria alveolata distribution and abundance curated through the REEHAB (REEf HABitat) Project* [Data set]. SEANOE. <https://doi.org/10.17882/72164>
- de la Hoz, C. F., Ramos, E., Puente, A., & Juanes, J. A. (2019). Temporal transferability of marine distribution models: The role of algorithm selection. *Ecological Indicators*, 106, 105499. <https://doi.org/10.1016/j.ecolind.2019.105499>
- Dubois, S., Retière, C., & Olivier, F. (2002). Biodiversity associated with Sabellaria alveolata (Polychaeta: Sabellariidae) reefs: effects of human disturbances. *Journal*

of the Marine Biological Association of the UK, 82(5), 817–826.

<https://doi.org/10.1017/S0025315402006185>

Egbert, G. D., & Erofeeva, S. Y. (2002). Efficient Inverse Modeling of Barotropic Ocean Tides. *Journal of Atmospheric and Oceanic Technology*, 19(2), 183–204.

[https://doi.org/10.1175/1520-0426\(2002\)019<0183:EIMOBO>2.0.CO;2](https://doi.org/10.1175/1520-0426(2002)019<0183:EIMOBO>2.0.CO;2)

Egbert, G. D., Erofeeva, S. Y., & Ray, R. D. (2010). Assimilation of altimetry data for nonlinear shallow-water tides: Quarter-diurnal tides of the Northwest European Shelf. *Continental Shelf Research*, 30(6), 668–679.

<https://doi.org/10.1016/j.csr.2009.10.011>

Elith*, J., H. Graham*, C., P. Anderson, R., Dudík, M., Ferrier, S., Guisan, A., J.

Hijmans, R., Huettmann, F., R. Leathwick, J., & Lehmann, A. (2006). Novel methods improve prediction of species' distributions from occurrence data.

Ecography, 29(2), 129–151.

Elith, J., Leathwick, J. R., & Hastie, T. (2008). A working guide to boosted regression trees. *Journal of Animal Ecology*, 77(4), 802–813.

Ellison, A. M., Bank, M. S., Clinton, B. D., Colburn, E. A., Elliott, K., Ford, C. R., Foster, D. R., Kloeppel, B. D., Knoepp, J. D., & Lovett, G. M. (2005). Loss of foundation species: Consequences for the structure and dynamics of forested ecosystems. *Frontiers in Ecology and the Environment*, 3(9), 479–486.

Estes, L., Elsen, P. R., Treuer, T., Ahmed, L., Caylor, K., Chang, J., Choi, J. J., & Ellis, E. C. (2018). The spatial and temporal domains of modern ecology. *Nature Ecology & Evolution*, 2(5), 819–826. <https://doi.org/10.1038/s41559-018-0524-4>

Faroni-Perez, L. (2017). Climate and environmental changes driving idiosyncratic shifts in the distribution of tropical and temperate worm reefs. *Journal of the Marine Biological Association of the United Kingdom*, 97(05), 1023–1035.

<https://doi.org/10.1017/S002531541700087X>

Firth, L. B., Mieszkowska, N., Grant, L. M., Bush, L. E., Davies, A. J., Frost, M. T., Moschella, P. S., Burrows, M. T., Cunningham, P. N., Dye, S. R., & Hawkins, S. J. (2015). Historical comparisons reveal multiple drivers of decadal change of an ecosystem engineer at the range edge. *Ecology and Evolution*, 5(15), 3210–3222.

<https://doi.org/10.1002/ece3.1556>

Firth, L. B., Harris, D., Blaze, J. A., Marzloff, M. P., Boyé, A., Miller, P. I., Curd, A., Vasquez, M., Nunn, J. D., O'Connor, N. E., Power, A. M., Mieszkowska, N., O'Riordan, R. M., Burrows, M. T., Bricheno, L. M., Knights, A. M., Nunes, F. L. D., Bordeyne, F., Bush, L. E., ... Hawkins, S. J. (2021a). Specific niche requirements underpin multidecadal range edge stability, but may introduce barriers for climate change adaptation. *Diversity and Distributions*, 27(4), 668–683.

<https://doi.org/10.1111/ddi.13224>

Firth, L. B., Curd, A., Hawkins, Stephen. J., Knights, A. M., Blaze, J. A., Burrows, M. T., Dubois, S. F., Edwards, H., Foggo, A., Gribben, P. E., Grant, L., Harris, D., Mieszkowska, N., Nunes, F. L. D., Nunn, J. D., Power, A. M., O'Riordan, R. M., McGrath, D., Simkanin, C., & O'Connor, N. E. (2021b). On the diversity and distribution of a data deficient habitat in a poorly mapped region: The case of *Sabellaria alveolata* L. in Ireland. *Marine Environmental Research*, 105344.

<https://doi.org/10.1016/j.marenvres.2021.105344>

- Frazier, A. E., & Kedron, P. (2017). Landscape Metrics: Past Progress and Future Directions. *Current Landscape Ecology Reports*, 2(3), 63–72.
<https://doi.org/10.1007/s40823-017-0026-0>
- Fredston-Hermann, A., Selden, R., Pinsky, M., Gaines, S. D., & Halpern, B. S. (2020). Cold range edges of marine fishes track climate change better than warm edges. *Global Change Biology*, 26(5), 2908–2922. <https://doi.org/10.1111/gcb.15035>
- Gaston, K. J. (1996). Species-range-size distributions: Patterns, mechanisms and implications. *Trends in Ecology & Evolution*, 11(5), 197–201.
- Génin, A., Majumder, S., Sankaran, S., Danet, A., Guttal, V., Schneider, F. D., & Kéfi, S. (2018). Monitoring ecosystem degradation using spatial data and the R package spatialwarnings. *Methods in Ecology and Evolution*, 9(10), 2067–2075.
<https://doi.org/10.1111/2041-210X.13058>
- Gribben, P. E., Angelini, C., Altieri, A. H., Bishop, M. J., Thomsen, M. S., & Bulleri, F. (2019). Facilitation cascades in marine ecosystems: A synthesis and future directions. In *Oceanography and Marine Biology*. Taylor & Francis.
- Guisan, A., Thuiller, W., & Zimmermann, N. E. (2017). *Habitat suitability and distribution models with applications in R*. Cambridge University Press.
- Hanley, J. A., & McNeil, B. J. (1982). The meaning and use of the area under a receiver operating characteristic (ROC) curve. *Radiology*, 143(1), 29-36.
- Hao, T., Elith, J., Lahoz-Monfort, J. J., & Guillera-Aroita, G. (2020). Testing whether ensemble modelling is advantageous for maximising predictive performance of species distribution models. *Ecography*, 43(4), 549–558.

- Harley, C. D. G., Randall Hughes, A., Hultgren, K. M., Miner, B. G., Sorte, C. J. B., Thornber, C. S., Rodriguez, L. F., Tomanek, L., & Williams, S. L. (2006). The impacts of climate change in coastal marine systems: Climate change in coastal marine systems. *Ecology Letters*, 9(2), 228–241. <https://doi.org/10.1111/j.1461-0248.2005.00871.x>
- Hastie, T., & Tibshirani, R. (1986). Generalized Additive Models. *Statistical Science*, 1(3). <https://doi.org/10.1214/ss/1177013604>
- Heikkinen, R. K., Marmion, M., & Luoto, M. (2012). Does the interpolation accuracy of species distribution models come at the expense of transferability? *Ecography*, 35(3), 276–288.
- Helmuth, B., Mieszkowska, N., Moore, P., & Hawkins, S. J. (2006). Living on the Edge of Two Changing Worlds: Forecasting the Responses of Rocky Intertidal Ecosystems to Climate Change. *Annual Review of Ecology, Evolution, and Systematics*, 37(1), 373–404. <https://doi.org/10.1146/annurev.ecolsys.37.091305.110149>
- Hesselbarth, M. H., Sciaini, M., With, K. A., Wiegand, K., & Nowosad, J. (2019). landscapemetrics: An open-source R tool to calculate landscape metrics. *Ecography*, 42(10), 1648–1657.
- Hesselbarth, M. H. K., Nowosad, J., Signer, J., & Graham, L. J. (2021). Open-source Tools in R for Landscape Ecology. *Current Landscape Ecology Reports*, 6(3), 97–111. <https://doi.org/10.1007/s40823-021-00067-y>

- Hijmans, R. J., Cameron, S. E., Parra, J. L., Jones, P. G., & Jarvis, A. (2005). Very high resolution interpolated climate surfaces for global land areas. *International Journal of Climatology*, 25(15), 1965–1978. <https://doi.org/10.1002/joc.1276>
- Howell, P. E., Muths, E., Hossack, B. R., Sigafus, B. H., & Chandler, R. B. (2018). Increasing connectivity between metapopulation ecology and landscape ecology. *Ecology*, 99(5), 1119–1128. <https://doi.org/10.1002/ecy.2189>
- Hutchinson, G. E. (1978). *An introduction to population ecology* (Issue 504: 51 HUT).
- Jones, A. G., Dubois, S. F., Desroy, N., & Fournier, J. (2018). Interplay between abiotic factors and species assemblages mediated by the ecosystem engineer *Sabellaria alveolata* (Annelida: Polychaeta). *Estuarine, Coastal and Shelf Science*, 200, 1–18. <https://doi.org/10.1016/j.ecss.2017.10.001>
- Kefi, S., Guttal, V., Brock, W. A., Carpenter, S. R., Ellison, A. M., Livina, V. N., Seekell, D. A., Scheffer, M., van Nes, E. H., & Dakos, V. (2014). Early warning signals of ecological transitions: Methods for spatial patterns. *PloS One*, 9(3), e92097.
- Lausch, A., Blaschke, T., Haase, D., Herzog, F., Syrbe, R.-U., Tischendorf, L., & Walz, U. (2015). Understanding and quantifying landscape structure – A review on relevant process characteristics, data models and landscape metrics. *Use of Ecological Indicators in Models*, 295, 31–41. <https://doi.org/10.1016/j.ecolmodel.2014.08.018>
- Lawson, C. R., Hodgson, J. A., Wilson, R. J., & Richards, S. A. (2014). Prevalence, thresholds and the performance of presence-absence models. *Methods in Ecology and Evolution*, 5(1), 54–64. <https://doi.org/10.1111/2041-210X.12123>

- Lemasson, A. J., Fletcher, S., Hall-Spencer, J. M. & Knights, A. M. (2017). Linking the biological impacts of ocean acidification on oysters to changes in ecosystem services: a review. *Journal of Experimental Marine Biology and Ecology*, 492, 49-62.
<https://doi.org/10.1016/j.jembe.2017.01.019>
- Lenoir, J., Bertrand, R., Comte, L., Bourgeaud, L., Hattab, T., Murienne, J., & Grenouillet, G. (2020). Species better track climate warming in the oceans than on land. *Nature Ecology & Evolution*, 4, 1044–1059. <https://doi.org/10.1038/s41559-020-1198-2>
- Lima, F. P., Ribeiro, P. A., Queiroz, N., Hawkins, S. J., & Santos, A. M. (2007). Do distributional shifts of northern and southern species of algae match the warming pattern? *Global Change Biology*, 13(12), 2592–2604.
- Lourenço, C. R., Nicastro, K. R., McQuaid, C. D., Krug, L. A., & Zardi, G. I. (2020). Strong upwelling conditions drive differences in species abundance and community composition along the Atlantic coasts of Morocco and Western Sahara. *Marine Biodiversity*, 50(2), 15. <https://doi.org/10.1007/s12526-019-01032-z>
- McCullagh, P., & Nelder, J. A. (1998). *Generalized linear models* (2nd ed). Chapman & Hall/CRC.
- Meinshausen, M., Smith, S. J., Calvin, K., Daniel, J. S., Kainuma, M., Lamarque, J.-F., Matsumoto, K., Montzka, S., Raper, S., & Riahi, K. (2011). The RCP greenhouse gas concentrations and their extensions from 1765 to 2300. *Climatic Change*, 109(1–2), 213.

Mestre, F., Risk, B. B., Mira, A., Beja, P., & Pita, R. (2017). A metapopulation approach to predict species range shifts under different climate change and landscape connectivity scenarios. *Ecological Modelling*, 359, 406–414.

Mieszkowska, N., Kendall, M., Hawkins, S., Leaper, R., Williamson, P., Hardman-Mountford, N., & Southward, A. (2006). Changes in the range of some common rocky shore species in Britain—A response to climate change? In *Marine Biodiversity* (pp. 241–251). Springer.

Mieszkowska, N., & Sugden, H. (2016). Climate-driven range shifts within benthic habitats across a marine biogeographic transition zone. *Advances in Ecological Research*, 55, 325–369.

Muir, A. P., Dubois, S. F., Ross, R. E., Firth, L. B., Knights, A. M., Lima, F. P., Seabra, R., Corre, E., Le Corguillé, G., & Nunes, F. L. D. (2020). Seascape genomics reveals population isolation in the reef-building honeycomb worm, *Sabellaria alveolata* (L.). *BMC Evolutionary Biology*, 20(1), 100.

<https://doi.org/10.1186/s12862-020-01658-9>

Naylor, L. A., & Viles, H. A. (2000). A temperate reef builder: An evaluation of the growth, morphology and composition of *Sabellaria alveolata* (L.) colonies on carbonate platforms in South Wales. *Geological Society, London, Special Publications*, 178(1), 9–19.

Newman, E. A., Kennedy, M. C., Falk, D. A., & McKenzie, D. (2019). Scaling and Complexity in Landscape Ecology. *Frontiers in Ecology and Evolution*, 7, 293.

<https://doi.org/10.3389/fevo.2019.00293>

- Nicastro, K. R., Zardi, G. I., Teixeira, S., Neiva, J., Serrão, E. A., & Pearson, G. A. (2013). Shift happens: Trailing edge contraction associated with recent warming trends threatens a distinct genetic lineage in the marine macroalga *Fucus vesiculosus*. *BMC Biology*, 11(1), 6. <https://doi.org/10.1186/1741-7007-11-6>
- Nijp, J. J., Temme, A. J. A. M., Voorn, G. A. K., Kooistra, L., Hengeveld, G. M., Soons, M. B., Teuling, A. J., & Wallinga, J. (2019). Spatial early warning signals for impending regime shifts: A practical framework for application in real-world landscapes. *Global Change Biology*, 25(6), 1905–1921. <https://doi.org/10.1111/gcb.14591>
- Nunes, F. L. D., Rigal, F., Dubois, S. F., & Viard, F. (2021). Looking for diversity in all the right places? Genetic diversity is highest in peripheral populations of the reef-building polychaete *Sabellaria alveolata*. *Marine Biology*, 168(5), 63. <https://doi.org/10.1007/s00227-021-03861-8>
- Opdam, P., & Wascher, D. (2004). Climate change meets habitat fragmentation: Linking landscape and biogeographical scale levels in research and conservation. *Biological Conservation*, 117(3), 285–297.
- Paquette, A., Hargreaves, A.L. (2021). Biotic interactions are more often important at species' warm versus cool range edges. *Ecology Letters* 24, 2427–2438. <https://doi.org/10.1111/ele.13864>
- Parmesan, C., & Yohe, G. (2003). A globally coherent fingerprint of climate change impacts across natural systems. *Nature*, 421(6918), 37–42.
- Pecl, G. T., Araújo, M. B., Bell, J. D., Blanchard, J., Bonebrake, T. C., Chen, I.-C., Clark, T. D., Colwell, R. K., Danielsen, F., Evengård, B., Falconi, L., Ferrier, S., Frusher,

- S., Garcia, R. A., Griffis, R. B., Hobday, A. J., Janion-Scheepers, C., Jarzyna, M. A., Jennings, S., ... Williams, S. E. (2017). Biodiversity redistribution under climate change: Impacts on ecosystems and human well-being. *Science*, 355(6332), eaai9214. <https://doi.org/10.1126/science.aai9214>
- Philippart, C. J. M., Anadón, R., Danovaro, R., Dippner, J. W., Drinkwater, K. F., Hawkins, S. J., Oguz, T., O'Sullivan, G., & Reid, P. C. (2011). Impacts of climate change on European marine ecosystems: Observations, expectations and indicators. *Journal of Experimental Marine Biology and Ecology*, 400(1–2), 52–69. <https://doi.org/10.1016/j.jembe.2011.02.023>
- Pinsky, M. L., Selden, R. L., & Kitchel, Z. J. (2020). Climate-Driven Shifts in Marine Species Ranges: Scaling from Organisms to Communities. *Annual Review of Marine Science*, 12(1), 153–179. <https://doi.org/10.1146/annurev-marine-010419-010916>
- Pither, J. (2003). Climate tolerance and interspecific variation in geographic range size. *Proceedings of the Royal Society of London. Series B: Biological Sciences*, 270(1514), 475–481. <https://doi.org/10.1098/rspb.2002.2275>
- Poloczanska, E. S., Burrows, M. T., Brown, C. J., García Molinos, J., Halpern, B. S., Hoegh-Guldberg, O., Kappel, C. V., Moore, P. J., Richardson, A. J., Schoeman, D. S., & Sydeman, W. J. (2016). Responses of Marine Organisms to Climate Change across Oceans. *Frontiers in Marine Science*, 3. <https://doi.org/10.3389/fmars.2016.00062>
- Poloczanska, E. S., Brown, C. J., Sydeman, W. J., Kiessling, W., Schoeman, D. S., Moore, P. J., Brander, K., Bruno, J. F., Buckley, L. B., Burrows, M. T., Duarte, C.

M., Halpern, B. S., Holding, J., Kappel, C. V., O'Connor, M. I., Pandolfi, J. M., Parmesan, C., Schwing, F., Thompson, S. A., & Richardson, A. J. (2013). Global imprint of climate change on marine life. *Nature Climate Change*, 3(10), 919–925. <https://doi.org/10.1038/nclimate1958>

Reiss, H., Cunze, S., König, K., Neumann, H., & Kröncke, I. (2011). Species distribution modelling of marine benthos: A North Sea case study. *Marine Ecology Progress Series*, 442, 71–86.

R Core Team. (2019). *R: A Language and Environment for Statistical Computing*. Vienna, Austria. Retrieved from <https://www.R-project.org/>

Richter, R. (1927). ‘Sandkorallen’—Riffe in der Nordsee. *Natur und Museum*, 57(2), 49–62.

Rocchini, D., Hortal, J., Lengyel, S., Lobo, J. M., Jimenez-Valverde, A., Ricotta, C., Bacaro, G., & Chiarucci, A. (2011). Accounting for uncertainty when mapping species distributions: The need for maps of ignorance. *Progress in Physical Geography*, 35(2), 211–226.

Salomon, J.-C., & Breton, M. (1993). An atlas of long-term currents in the Channel. *Oceanologica Acta*, 16(5), 439–448.

Schindler, S., von Wehrden, H., Poirazidis, K., Wrbka, T., & Kati, V. (2013). Multiscale performance of landscape metrics as indicators of species richness of plants, insects and vertebrates. *Linking Landscape Structure and Biodiversity*, 31, 41–48. <https://doi.org/10.1016/j.ecolind.2012.04.012>

Schmitt, S., Pouteau, R., Justeau, D., Boissieu, F., & Birnbaum, P. (2017). SSDM: An R package to predict distribution of species richness and composition based on

- stacked species distribution models. *Methods in Ecology and Evolution*, 8(12), 1795–1803. <https://doi.org/10.1111/2041-210X.12841>
- Seabra, R., Varela, R., Santos, A. M., Gómez-Gesteira, M., Meneghesso, C., Wetthey, D. S., & Lima, F. P. (2019). Reduced Nearshore Warming Associated With Eastern Boundary Upwelling Systems. *Frontiers in Marine Science*, 6, 104. <https://doi.org/10.3389/fmars.2019.00104>
- Sillero, N., & Barbosa, A. M. (2021). Common mistakes in ecological niche models. *International Journal of Geographical Information Science*, 35(2), 213–226. <https://doi.org/10.1080/13658816.2020.1798968>
- Steen, V. A., Tingley, M. W., Paton, P. W., & Elphick, C. S. (2021). Spatial thinning and class balancing: Key choices lead to variation in the performance of species distribution models with citizen science data. *Methods in Ecology and Evolution*, 12(2), 216–226.
- Somero, G. (2010). The physiology of climate change: How potentials for acclimatization and genetic adaptation will determine ‘winners’ and ‘losers’. *Journal of Experimental Biology*, 213(6), 912–920.
- Sunday, J. M., Bates, A. E., & Dulvy, N. K. (2012). Thermal tolerance and the global redistribution of animals. *Nature Climate Change*, 2(9), 686–690.
- Thomas, C. D. (2010). Climate, climate change and range boundaries: Climate and range boundaries. *Diversity and Distributions*, 16(3), 488–495. <https://doi.org/10.1111/j.1472-4642.2010.00642.x>
- Thuiller, W. (2004). Patterns and uncertainties of species’ range shifts under climate change. *Global Change Biology*, 10(12), 2020–2027.

- Thuiller, W., Lafourcade, B., Engler, R., & Araújo, M. B. (2009). BIOMOD—a platform for ensemble forecasting of species distributions. *Ecography*, 32(3), 369–373.
- Tolman, H. L. (2009). User manual and system documentation of WAVEWATCH III TM version 3.14. *Technical Note, MMAB Contribution*, 276, 220.
- Turner, M. G. (2005). Landscape Ecology: What is the State of the Science? *Annual Review of Ecology, Evolution, and Systematics*, 36, 319–344.
<http://www.jstor.org/stable/30033807>
- Tyberghein, L., Verbruggen, H., Pauly, K., Troupin, C., Mineur, F., & De Clerck, O. (2012). Bio-ORACLE: A global environmental dataset for marine species distribution modelling: Bio-ORACLE marine environmental data rasters. *Global Ecology and Biogeography*, 21(2), 272–281. <https://doi.org/10.1111/j.1466-8238.2011.00656.x>
- Uuemaa, E., Mander, Ü., & Marja, R. (2013). Trends in the use of landscape spatial metrics as landscape indicators: A review. *10 Years Ecological Indicators*, 28, 100–106. <https://doi.org/10.1016/j.ecolind.2012.07.018>
- VanDerWal, J., Murphy, H. T., Kutt, A. S., Perkins, G. C., Bateman, B. L., Perry, J. J., & Reside, A. E. (2013). Focus on poleward shifts in species' distribution underestimates the fingerprint of climate change. *Nature Climate Change*, 3(3), 239–243. <https://doi.org/10.1038/nclimate1688>
- Wallingford, P. D., Morelli, T. L., Allen, J. M., Beaury, E. M., Blumenthal, D. M., Bradley, B. A., Dukes, J. S., Early, R., Fusco, E. J., Goldberg, D. E., Ibáñez, I., Laginhas, B. B., Vilà, M., & Sorte, C. J. B. (2020). Adjusting the lens of invasion

- biology to focus on the impacts of climate-driven range shifts. *Nature Climate Change*. <https://doi.org/10.1038/s41558-020-0768-2>
- Walther, G.-R. (2010). Community and ecosystem responses to recent climate change. *Philosophical Transactions of the Royal Society B: Biological Sciences*, 365(1549), 2019–2024. <https://doi.org/10.1098/rstb.2010.0021>
- Wenger, S. J., & Olden, J. D. (2012). Assessing transferability of ecological models: An underappreciated aspect of statistical validation. *Methods in Ecology and Evolution*, 3(2), 260–267.
- Wethey, D. S., Woodin, S. A., Hilbish, T. J., Jones, S. J., Lima, F. P., & Brannock, P. M. (2011). Response of intertidal populations to climate: Effects of extreme events versus long term change. *Journal of Experimental Marine Biology and Ecology*, 400(1–2), 132–144. <https://doi.org/10.1016/j.jembe.2011.02.008>
- Wilson, D. P. (1971). Sabellaria Colonies At Duckpool, North Cornwall, 1961–1970. *Journal of the Marine Biological Association of the United Kingdom*, 51(03), 509. <https://doi.org/10.1017/S002531540001496X>
- Wort, E. J., Chapman, M. A., Hawkins, S. J., Henshall, L., Pita, A., Rius, M., Williams, S. T., & Fenberg, P. B. (2019). Contrasting genetic structure of sympatric congeneric gastropods: Do differences in habitat preference, abundance and distribution matter? *Journal of Biogeography*, 46(2), 369–380.
- Wright, J. P. (2009). Linking populations to landscapes: Richness scenarios resulting from changes in the dynamics of an ecosystem engineer. *Ecology*, 90(12), 3418–3429.

Yalcin, S., & Leroux, S. J. (2017). Diversity and suitability of existing methods and metrics for quantifying species range shifts. *Global Ecology and Biogeography*, 26(6), 609–624.

Yates, K. L., Bouchet, P. J., Caley, M. J., Mengersen, K., Randin, C. F., Parnell, S., Fielding, A. H., Bamford, A. J., Ban, S., & Barbosa, A. M. (2018). Outstanding challenges in the transferability of ecological models. *Trends in Ecology & Evolution*, 33(10), 790–802.

Supplementary Information for

Applying landscape metrics to species distribution model predictions to characterise internal range structure and associated changes

Amelia Curd, Mathieu Chevalier, Mickaël Vasquez, Aurélien Boyé, Louise B. Firth, Martin P. Marzloff, Lucy M. Bricheno, Michael T. Burrows, Laura E. Bush, Céline Cordier, Andrew J. Davies, J.A. Mattias Green, Stephen J. Hawkins, Fernando P. Lima, Claudia Meneghesso, Nova Mieszkowska, Rui Seabra and Stanislas F. Dubois

Amelia Curd

Email: amelia.curd@ifremer.fr

This PDF file includes:

Supplementary text

Figures S1 to S13

Tables S1 to S5

Pre-proof of Curd et al. 2023. Applying landscape metrics to species distribution model predictions to characterize internal range structure and associated changes. *Global Change Biology*, 29: 631-647. Please visit <https://onlinelibrary.wiley.com/doi/full/10.1111/gcb.16496> for final version.

Supplementary Information Text

Evolutionary consequences of increasingly isolated peripheral populations. Range edges are characterized by variable and unstable conditions, relative to the range center (Pironon et al., 2017). It is likely that peripheral populations evolve resistance to extreme conditions. Therefore, those reefs in the center-region may be subject to more environmental stability than at the edges, making individuals less adaptable, which may in turn lead to greater climatic sensitivity. High *S. alveolata* abundance creates large reefs such as those found on the center-region peak on Oléron island, France, which further buffer and stabilize their environment, possibly rendering individuals found in large bioconstructions even less adaptable (Dubois, unpublished data). Range edge populations are expected to be genetically more variable, since changeable conditions induce a fluctuating selection, which maintains high genetic diversity (Bridle & Vines, 2007). A phylogeographic study has revealed *S. alveolata* genetic diversity to be highest in the Irish Sea and the English Channel, and relatively high in Morocco compared to the Bay of Biscay (Nunes et al., 2021). Range edge populations rather than central ones may therefore be more resistant to environmental extremes and changes, and should be treated as a biogenetic resource used for rehabilitation and restoration of damaged ecosystems. The populations of *S. alveolata* at both range edges should be conserved now as potentially resilient genetic repositories, to be used in the future for mitigating undesirable effects of global climate change.

Realism and accuracy of model projections. The projections we make contain several sources of uncertainty, which future research could help resolve. For example, we do not account for substrate or larval dispersal, which could change the ecological significance of our results (Cecino et al., 2021). If present-day larval dispersal boundaries are not breached (Wethey et al., 2011), this will result in large areas of potentially suitable habitat, particularly along the extensive coastline of western Scotland, remaining unoccupied, leading to an overall net loss in suitable habitat area. If and once larvae reach a new area of suitable habitat, they require a suitable hard substrate on which to settle (Pawlik, 1988). Hard substrate was not included in our model, as detailed intertidal rock data measured or modelled over large geographic gradients is unavailable. Nevertheless, our model performed well, as demonstrated by the correlation between the high-abundance areas and the peaks in habitat suitability (see *SI Appendix* Fig. S2 and S7a). It should however be noted that *S. alveolata* settles well on artificial hard substrates. The proliferation of artificial coastlines is expected to increase suitable area for *S. alveolata*, however this was impossible to quantitatively predict with our approach.

Another source of uncertainty is that of short-term extreme climatic events (Morán-Ordóñez et al., 2018). All six environmental predictors used in our analyses are averaged over a decade or more, and may not represent the critical bottlenecks for long-term species persistence (Sunday et al.,

2012). As an example, there are predicted significant increases in marine heatwave intensity and count of annual marine heatwave days are projected to accelerate (Oliver et al., 2021). Their effect will depend on how *S.alveolata* responds, but especially which populations are affected. Possible scenarios include accelerated extirpations at the trailing edge due to heatwaves, slowed poleward migration and diminished survival at the leading edge due to cold snaps and center-range extreme events which could create a dispersal break between populations.

A final critical underlying assumption in biogeographic modelling is that of stationarity or niche conservatism in space and time, i.e. that predictions made on the basis of one location and time will be valid in other geographic regions at other times (Woodin et al., 2013). Were local populations to become adapted in the future, with consequent shifts in the Grinnellian niche (Miller, 2010; Waltari & Hickerson, 2013), SDM transferability would not be possible. Nonetheless, our estimates provide a first global assessment of the effects of climate change on an intertidal engineered habitat on which future refinements can build.

References

- Bridle, J. R., & Vines, T. H. (2007). Limits to evolution at range margins: When and why does adaptation fail? *Trends in Ecology & Evolution*, 22(3), 140–147.
- Cecino, G., Valavi, R., & Treml, E. A. (2021). Testing the Influence of Seascape Connectivity on Marine-Based Species Distribution Models. *Frontiers in Marine Science*, 8, 766915. <https://doi.org/10.3389/fmars.2021.766915>
- Miller, J. (2010). Species Distribution Modeling: Species distribution modeling. *Geography Compass*, 4(6), 490–509. <https://doi.org/10.1111/j.1749-8198.2010.00351.x>
- Morán-Ordóñez, A., Briscoe, N. J., & Wintle, B. A. (2018). Modelling species responses to extreme weather provides new insights into constraints on range and likely climate change

impacts for Australian mammals. *Ecography*, 41(2), 308–320.

<https://doi.org/10.1111/ecog.02850>

Nunes, F. L. D., Rigal, F., Dubois, S. F., & Viard, F. (2021). Looking for diversity in all the right places? Genetic diversity is highest in peripheral populations of the reef-building polychaete *Sabellaria alveolata*. *Marine Biology*, 168(5), 63.

<https://doi.org/10.1007/s00227-021-03861-8>

Oliver, E. C., Benthuisen, J. A., Darmaraki, S., Donat, M. G., Hobday, A. J., Holbrook, N. J., Schlegel, R. W., & Sen Gupta, A. (2021). Marine heatwaves. *Annual Review of Marine Science*, 13, 313–342.

Pawlik, J. R. (1988). Larval settlement and metamorphosis of sabellariid polychaetes, with special reference to *Phragmatopoma lapidosa*, a reef-building species, and *Sabellaria floridensis*, a non-gregarious species. *Bulletin of Marine Science*, 43(1), 41–60.

Pironon, S., Papuga, G., Villellas, J., Angert, A. L., García, M. B., & Thompson, J. D. (2017). Geographic variation in genetic and demographic performance: New insights from an old biogeographical paradigm: The centre-periphery hypothesis. *Biological Reviews*, 92(4), 1877–1909. <https://doi.org/10.1111/brv.12313>

Sunday, J. M., Bates, A. E., & Dulvy, N. K. (2012). Thermal tolerance and the global redistribution of animals. *Nature Climate Change*, 2(9), 686–690.

Waltari, E., & Hickerson, M. J. (2013). Late Pleistocene species distribution modelling of North Atlantic intertidal invertebrates. *Journal of Biogeography*, 40(2), 249–260.

<https://doi.org/10.1111/j.1365-2699.2012.02782.x>

Wethey, D. S., Woodin, S. A., Hilbish, T. J., Jones, S. J., Lima, F. P., & Brannock, P. M. (2011). Response of intertidal populations to climate: Effects of extreme events versus long term change. *Journal of Experimental Marine Biology and Ecology*, 400(1–2), 132–144.

<https://doi.org/10.1016/j.jembe.2011.02.008>

Woodin, S. A., Hilbish, T. J., Helmuth, B., Jones, S. J., & Wethey, D. S. (2013). Climate change, species distribution models, and physiological performance metrics: Predicting when

Pre-proof of Curd et al. 2023. Applying landscape metrics to species distribution model predictions to characterize internal range structure and associated changes. *Global Change Biology*, 29: 631-647. Please visit <https://onlinelibrary.wiley.com/doi/full/10.1111/gcb.16496> for final version.

biogeographic models are likely to fail. *Ecology and Evolution*, n/a-n/a.

<https://doi.org/10.1002/ece3.680>

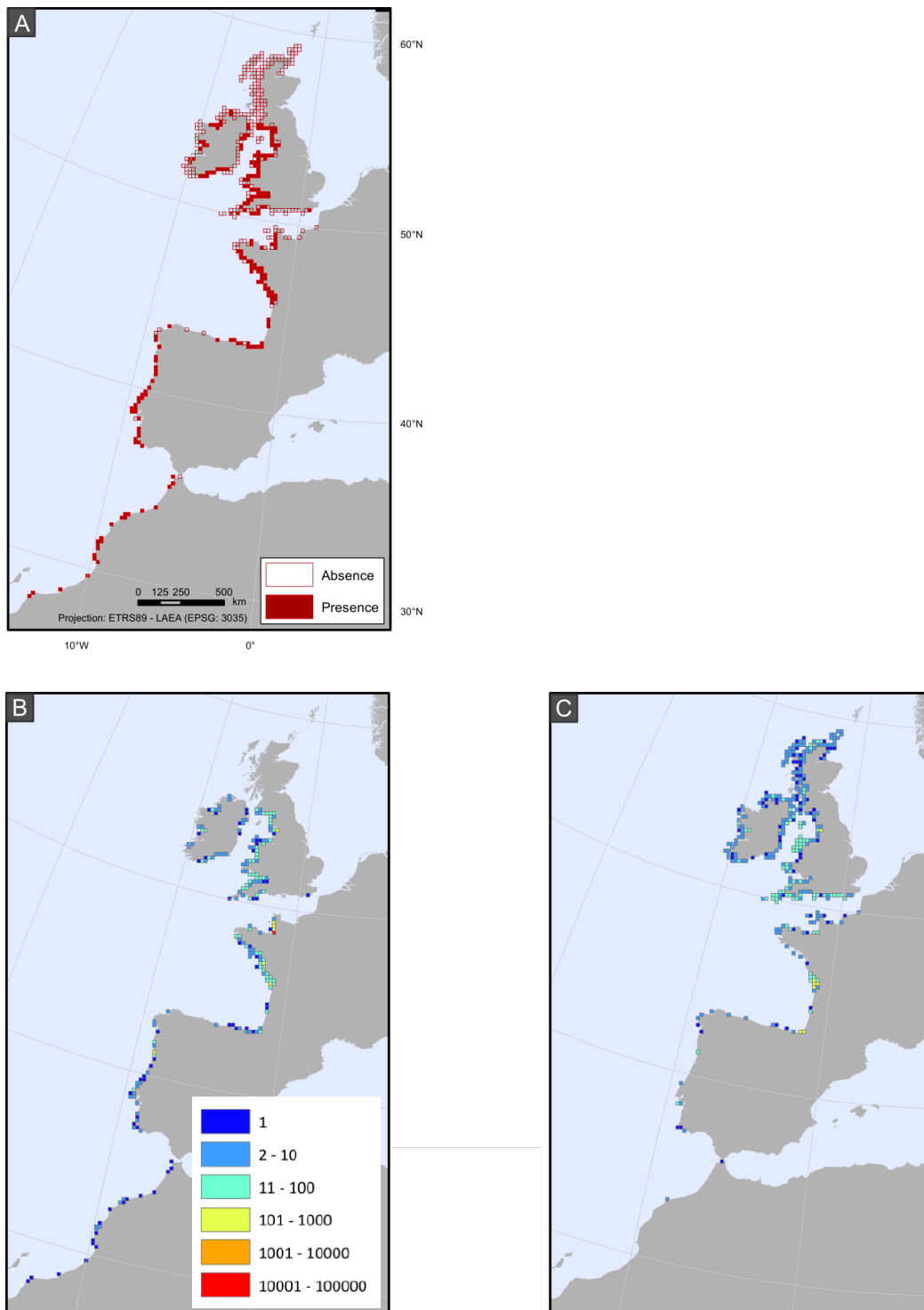


Figure S1. Maps illustrating the distribution and density of the 19354 collated *Sabellaria alveolata* records along the North-east Atlantic coast, where **A**) shows presence (filled squares) and absence

(open squares) records projected onto a 20km grid cell; **B**) the density of the 14960 presence records per 20km grid cell according to a log base 10 scale; **C**) the density of the 4394 absence records per 20km grid cell according to a log base 10 scale. Given the uneven geographic spread in absence records and imbalance between the number of presence and absence records, we chose to run a presence/pseudo-absence model.

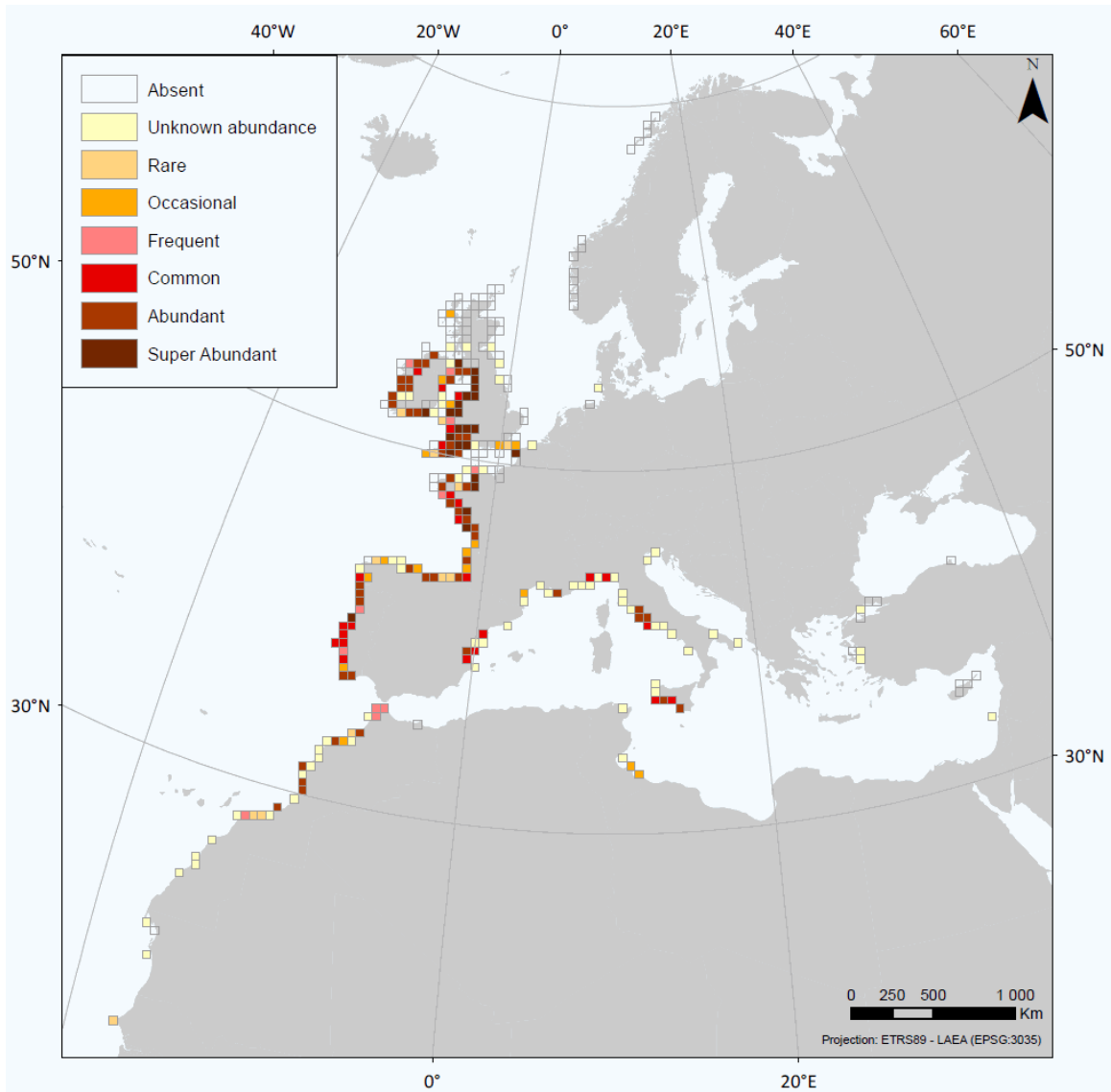


Figure S2. *Sabellaria alveolata* records projected onto a 50km grid. When SACFOR scale abundance scores were given to occurrence records, the highest abundance value per grid cell was retained. For more information see <https://www.seaone.org/data/00610/72164/>

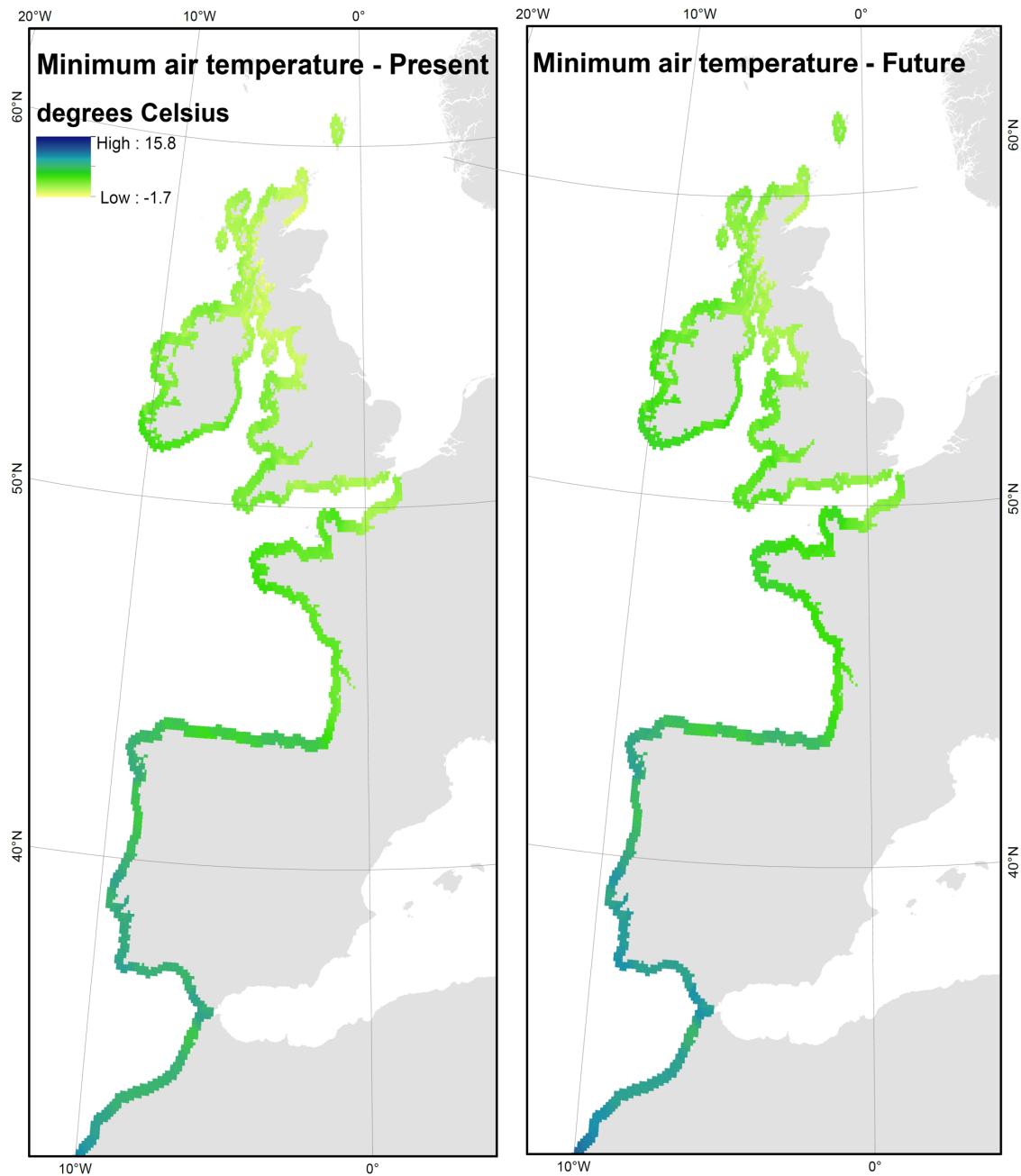


Figure S3. Maps of the minimum air temperature variable (one of six selected environmental variables retained as our SDM predictors), used to explain present-day and future (RCP4.5 2050) species distribution.

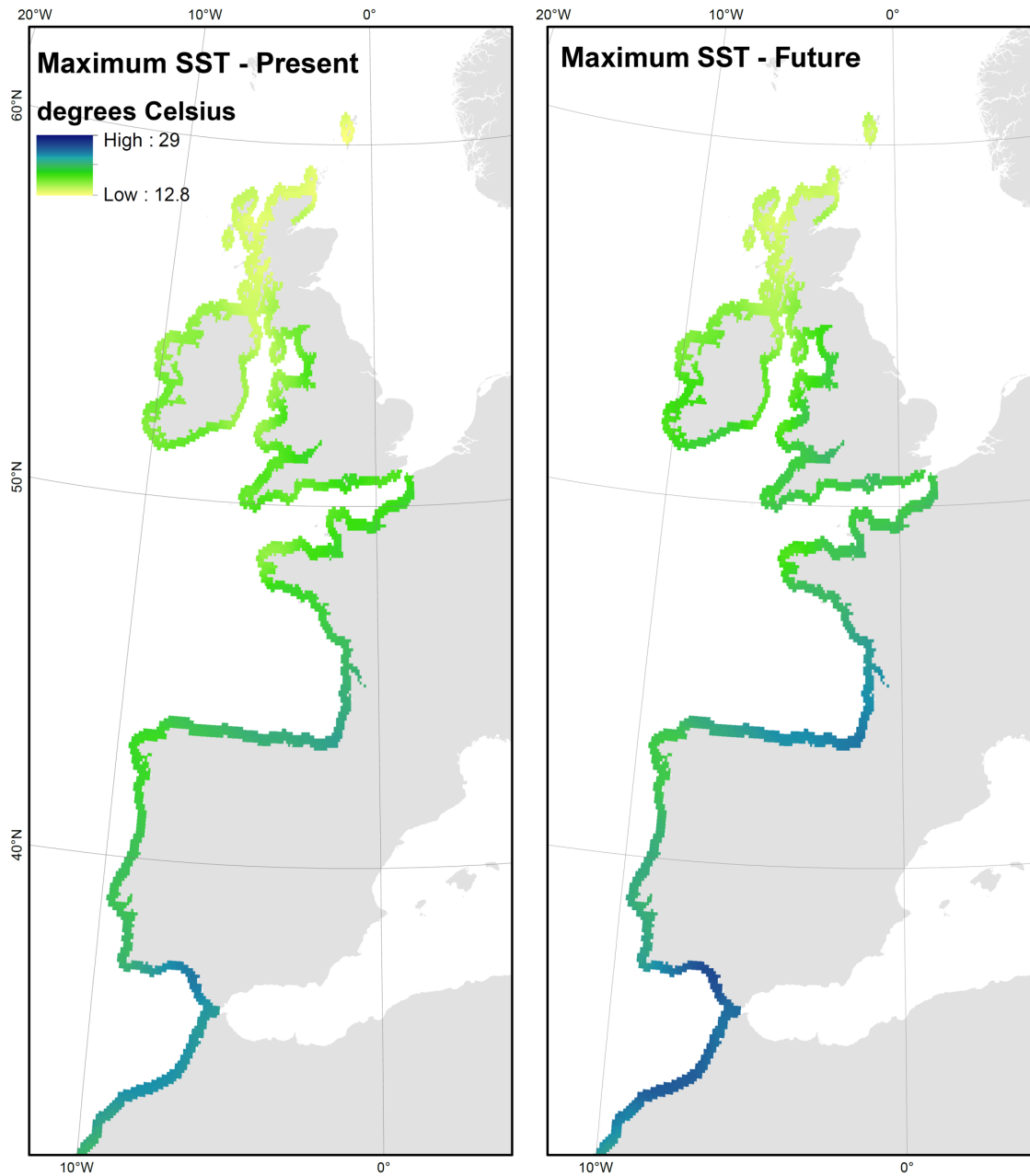


Figure S4. Maps of the maximum Sea Surface Temperature (SST) (one of six selected environmental variables retained as our SDM predictors), used to explain present-day and future (RCP4.5 2050) species distribution.

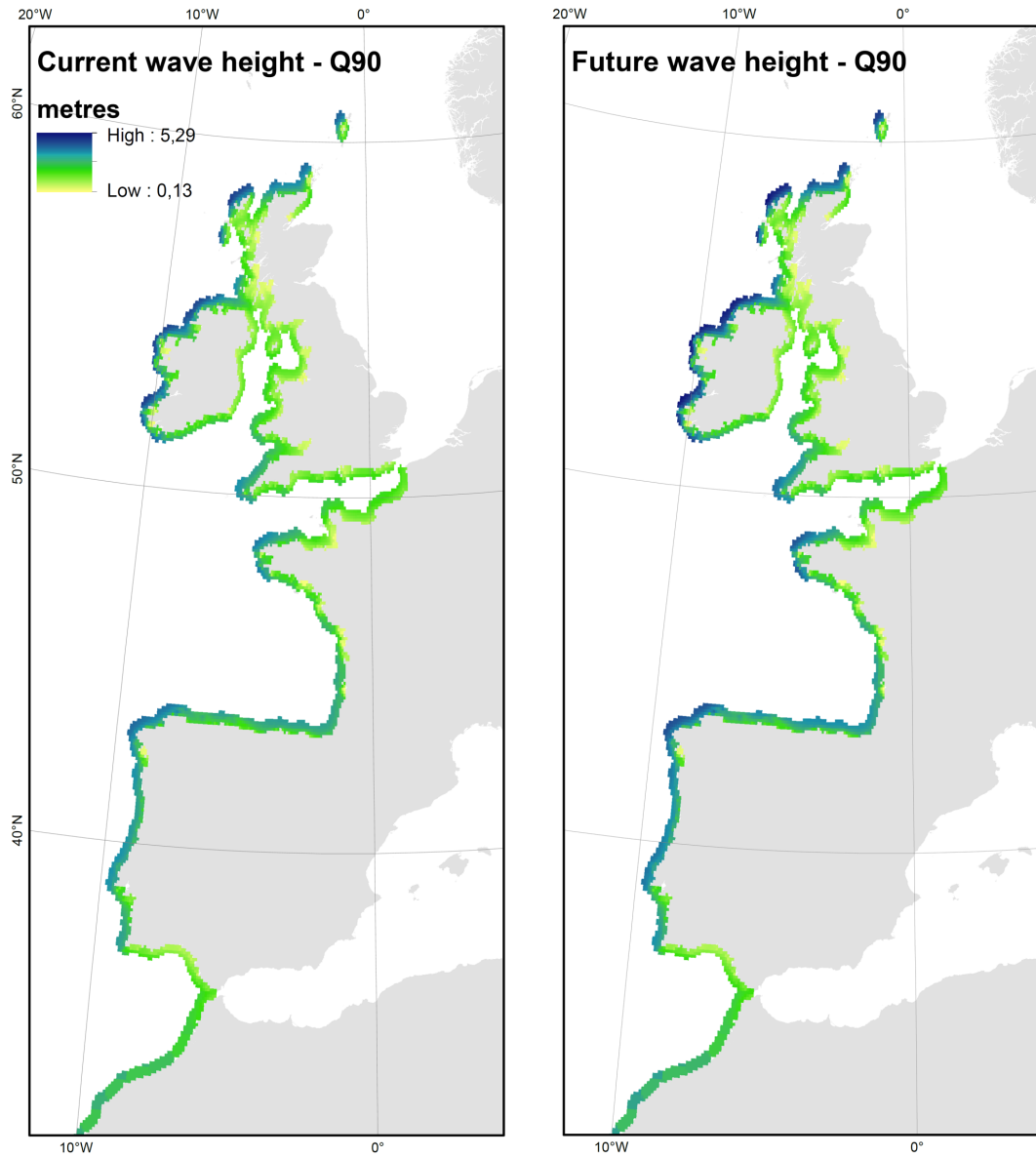


Figure S5. Maps of the 90th percentile of significant wave height (one of six selected environmental variables retained as our SDM predictors), used to explain present-day and future (RCP4.5 2050) species distribution.

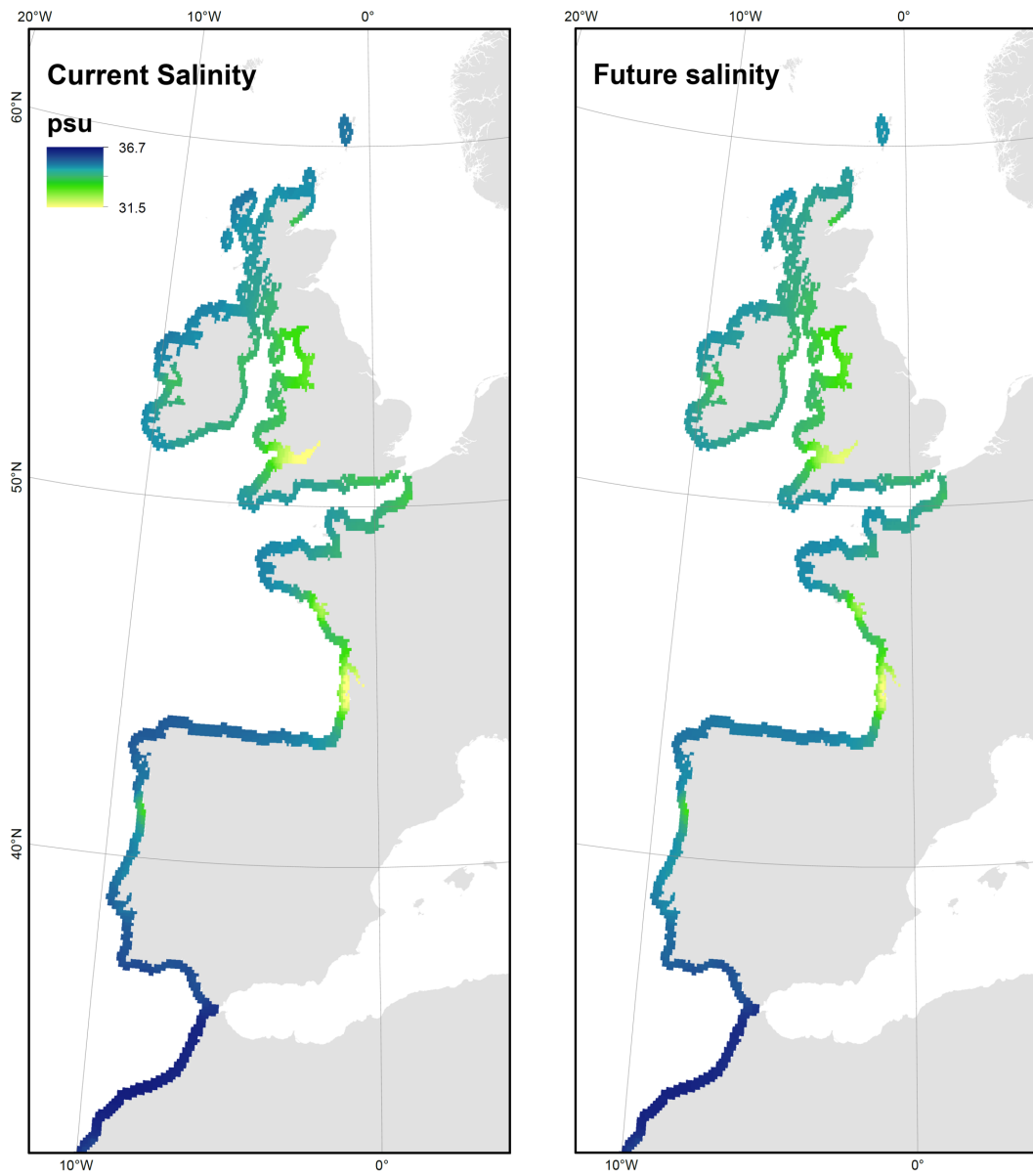


Figure S6. Maps of mean salinity (one of six selected environmental variables retained as our SDM predictors), used to explain present-day and future (RCP4.5 2050) species distribution.

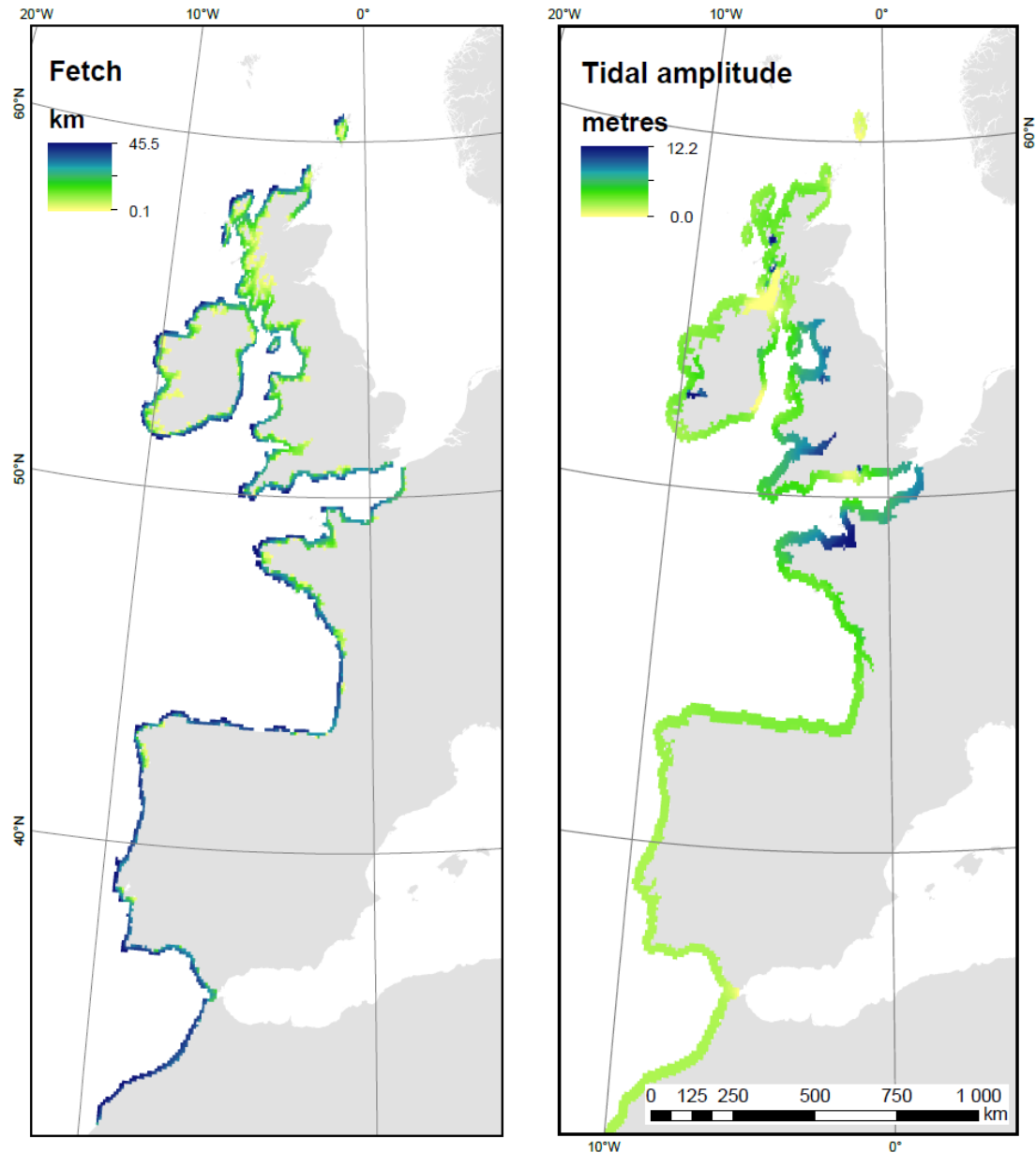


Figure S7. Maps of fetch and tidal amplitude (two of six selected environmental variables retained as our SDM predictors), used to explain present-day and future (RCP4.5 2050) species distribution. Note that fetch and tidal amplitude are considered to not vary, so that the same values are used in both time periods.

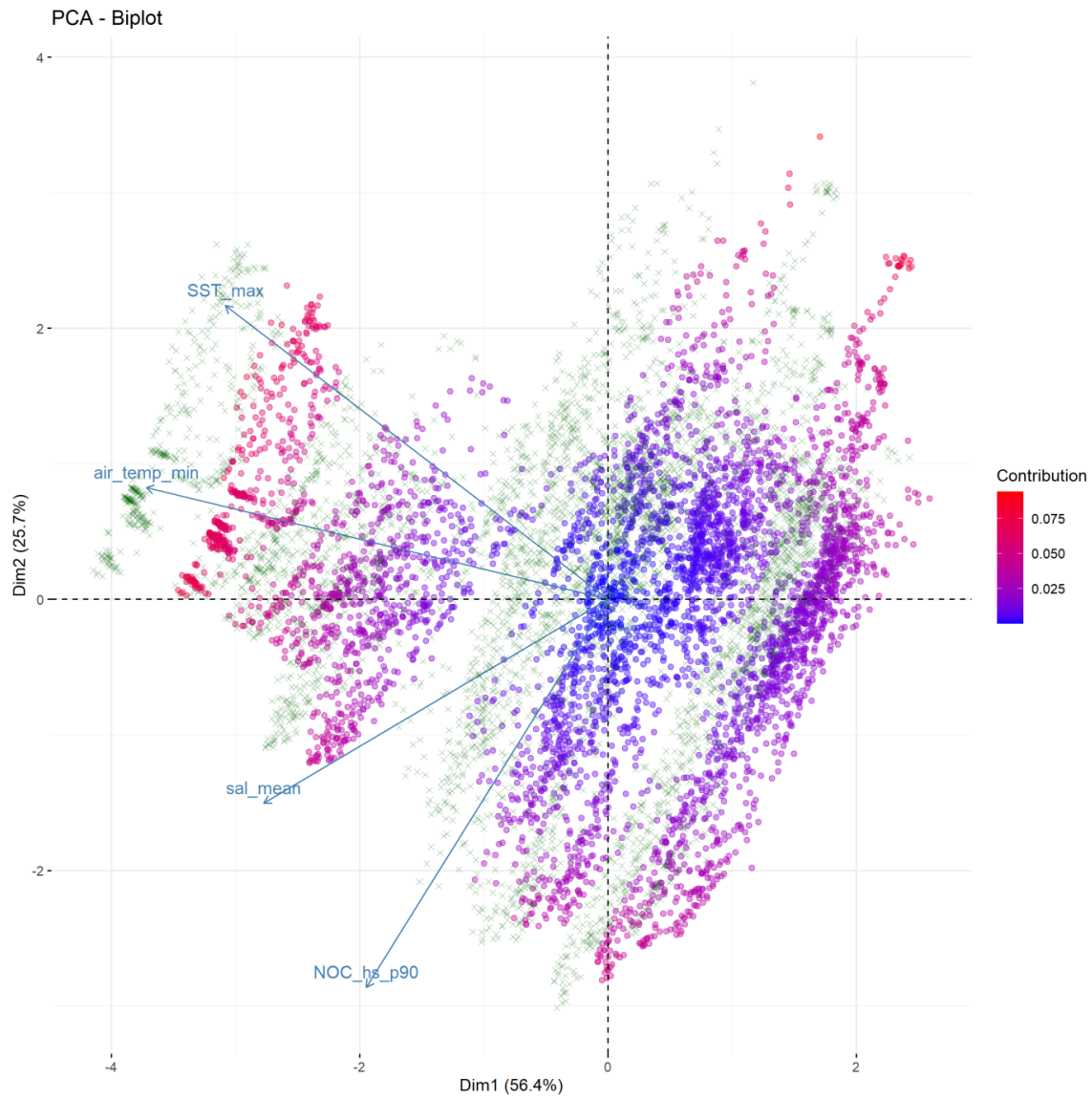


Figure S8. Principal Component Analysis (PCA) biplot performed on the current environmental conditions (4 variables) of 4721 pixels encompassing the whole distribution of the study species and over which current and future predictions were performed. The first two dimensions of the PCA express 82.1% of the total dataset inertia. The blue vectors indicate the current environmental variables: NOC_hs_p90 = 90th percentile wave height; sal_mean = mean salinity; air_temp_min = minimum air temperature; SST_max = maximum sea surface temperature. Green crosses highlight the future value of the pixels and demonstrate a shift along the first PCA axis towards higher temperatures. The PCA was performed using the package *ade4* (Bougeard & Dray, 2018) in R.

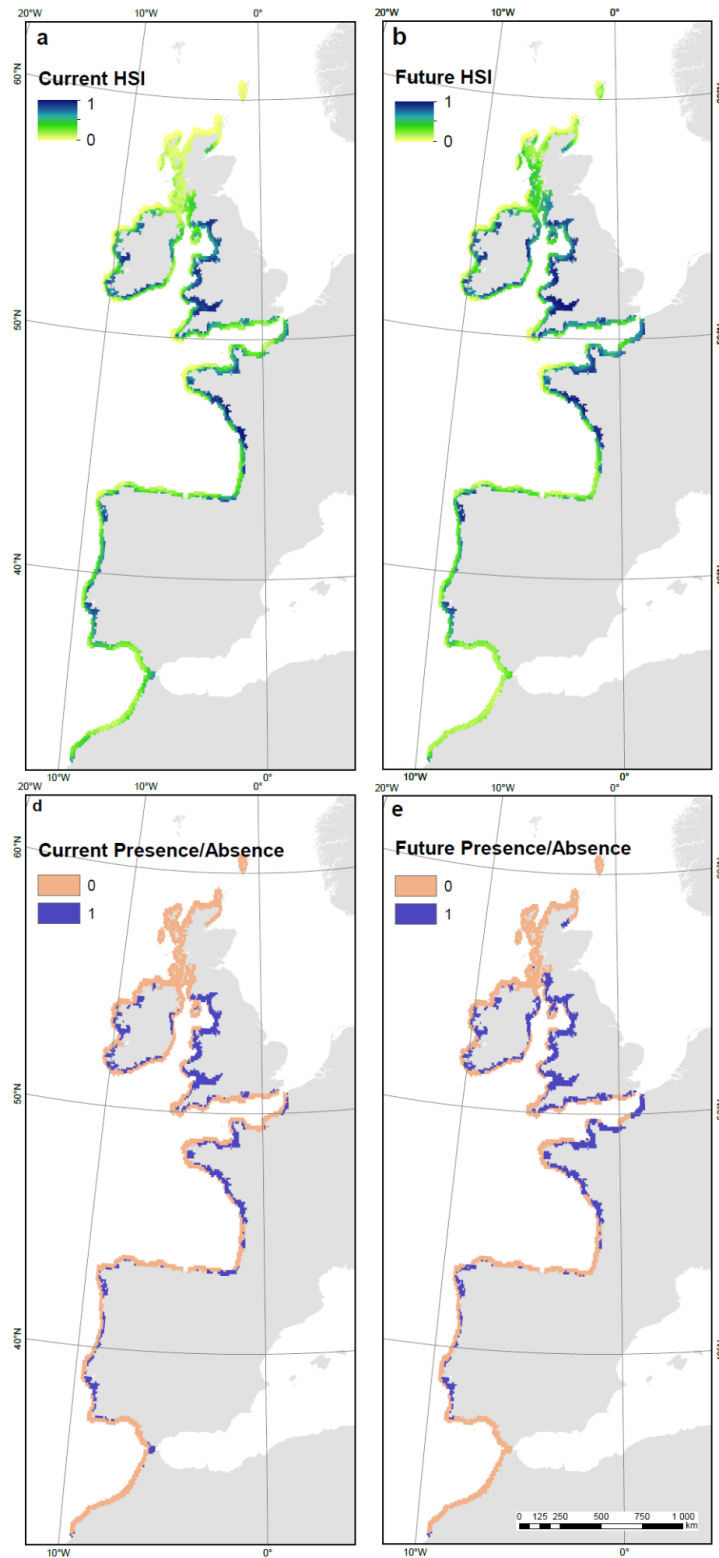


Figure S9. Predicted maps of the current and future Habitat Suitability Index (HSI 9a & 9b) and binary presence/absence (9d & 9e).

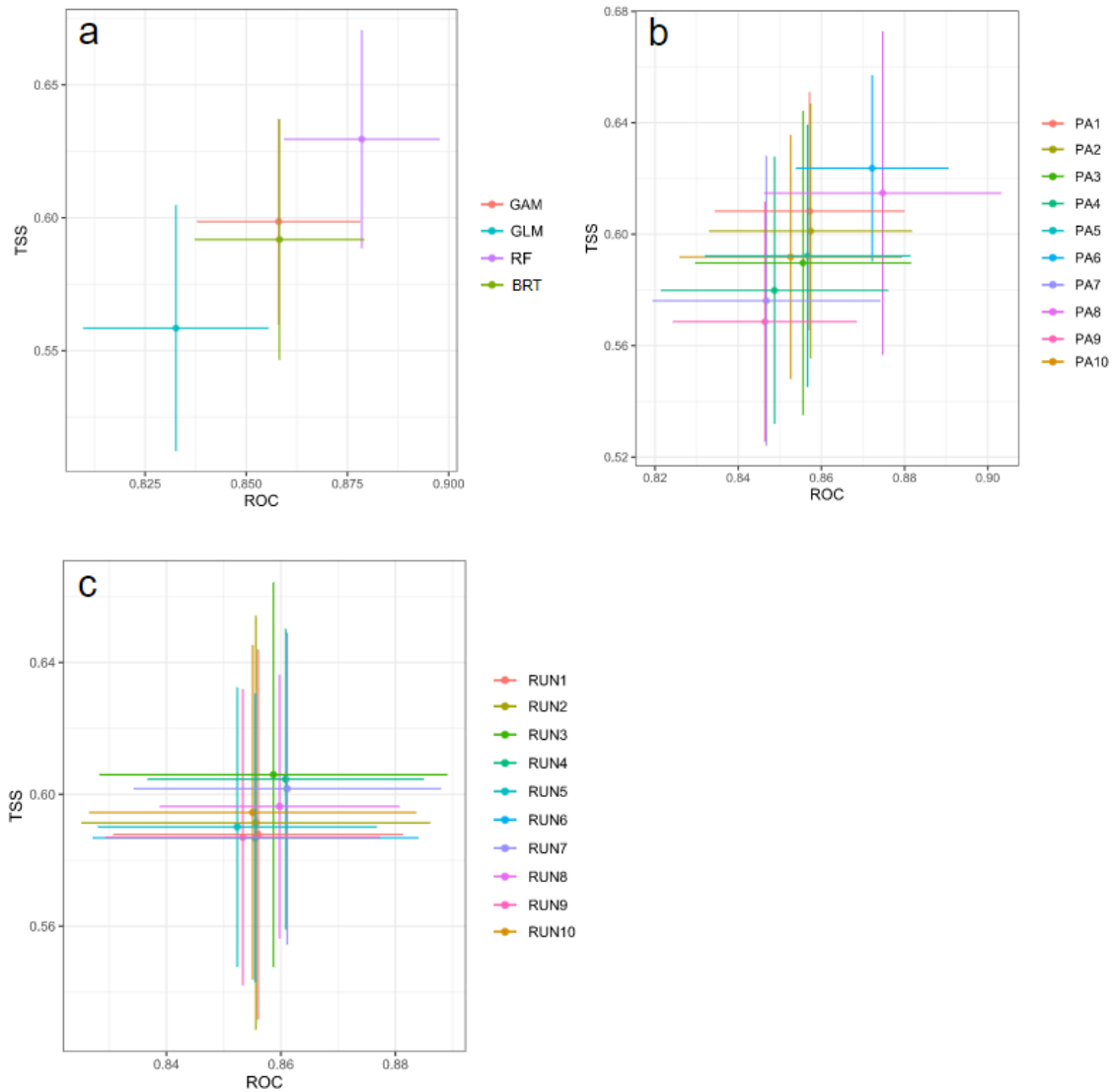


Figure S10. True Skill Statistic (TSS) and area under the Receiving Operator Characteristic (ROC) curve values for **a)** all four algorithms **b)** all ten presence/pseudo-absence runs and **c)** all ten model runs.

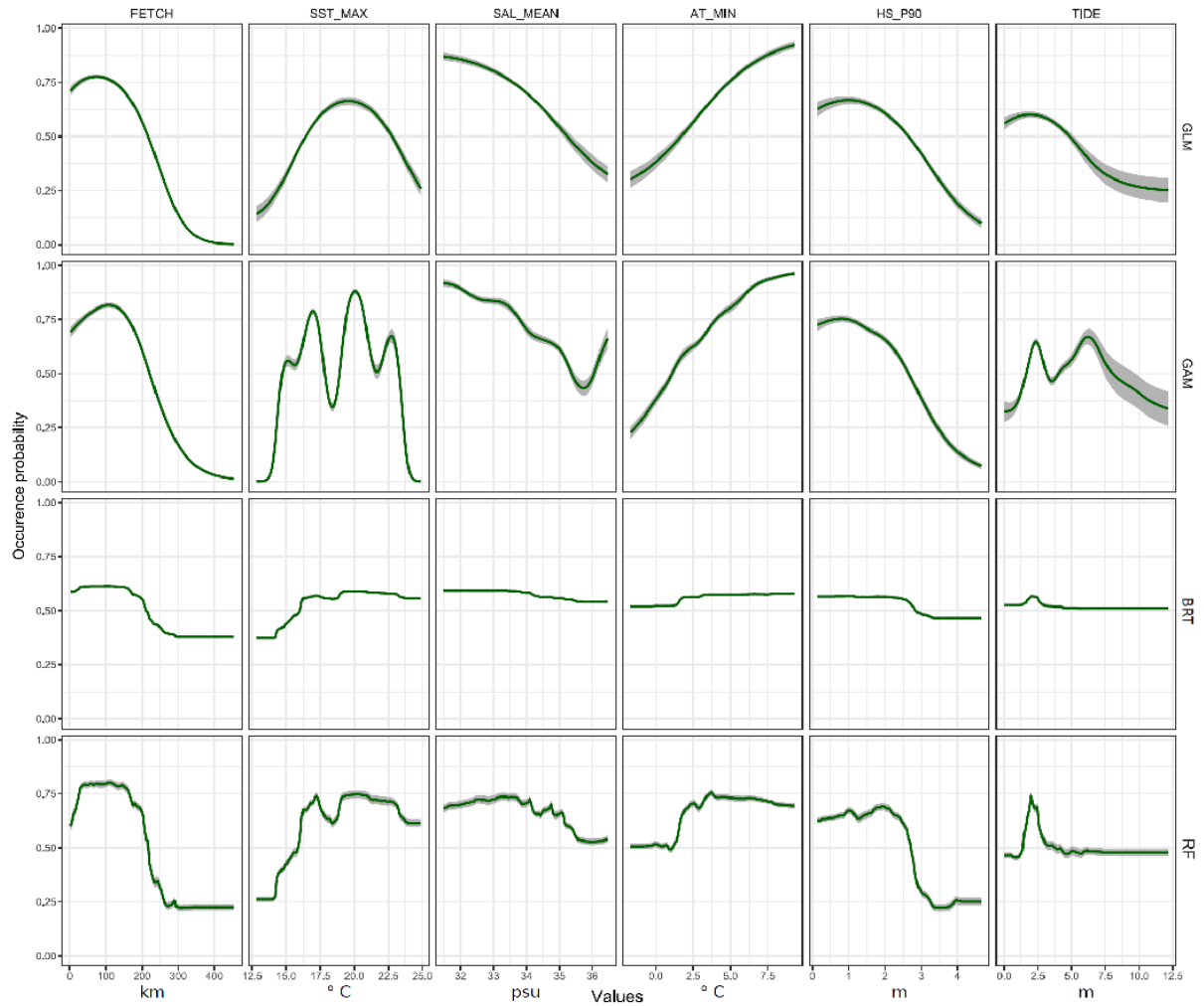
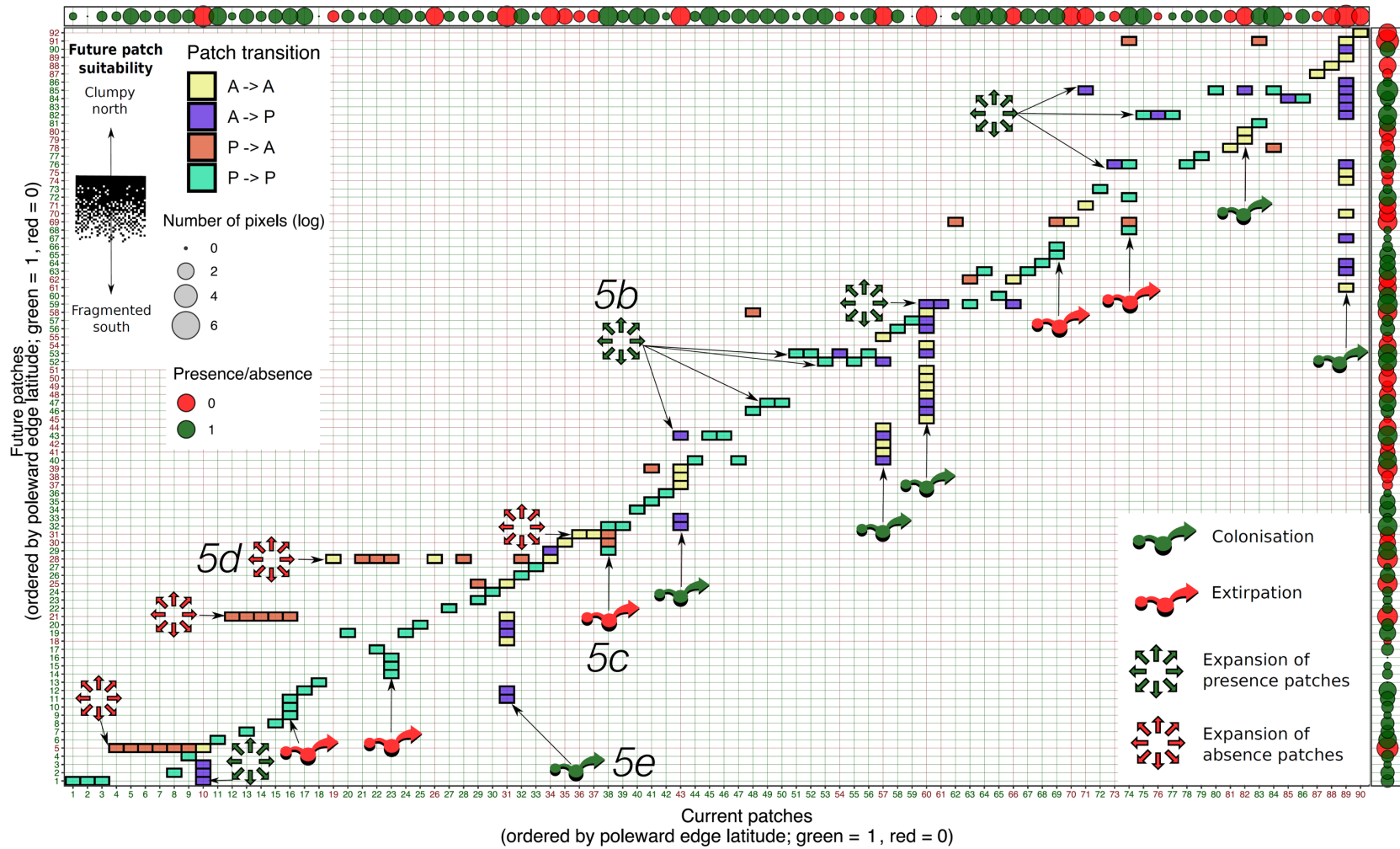
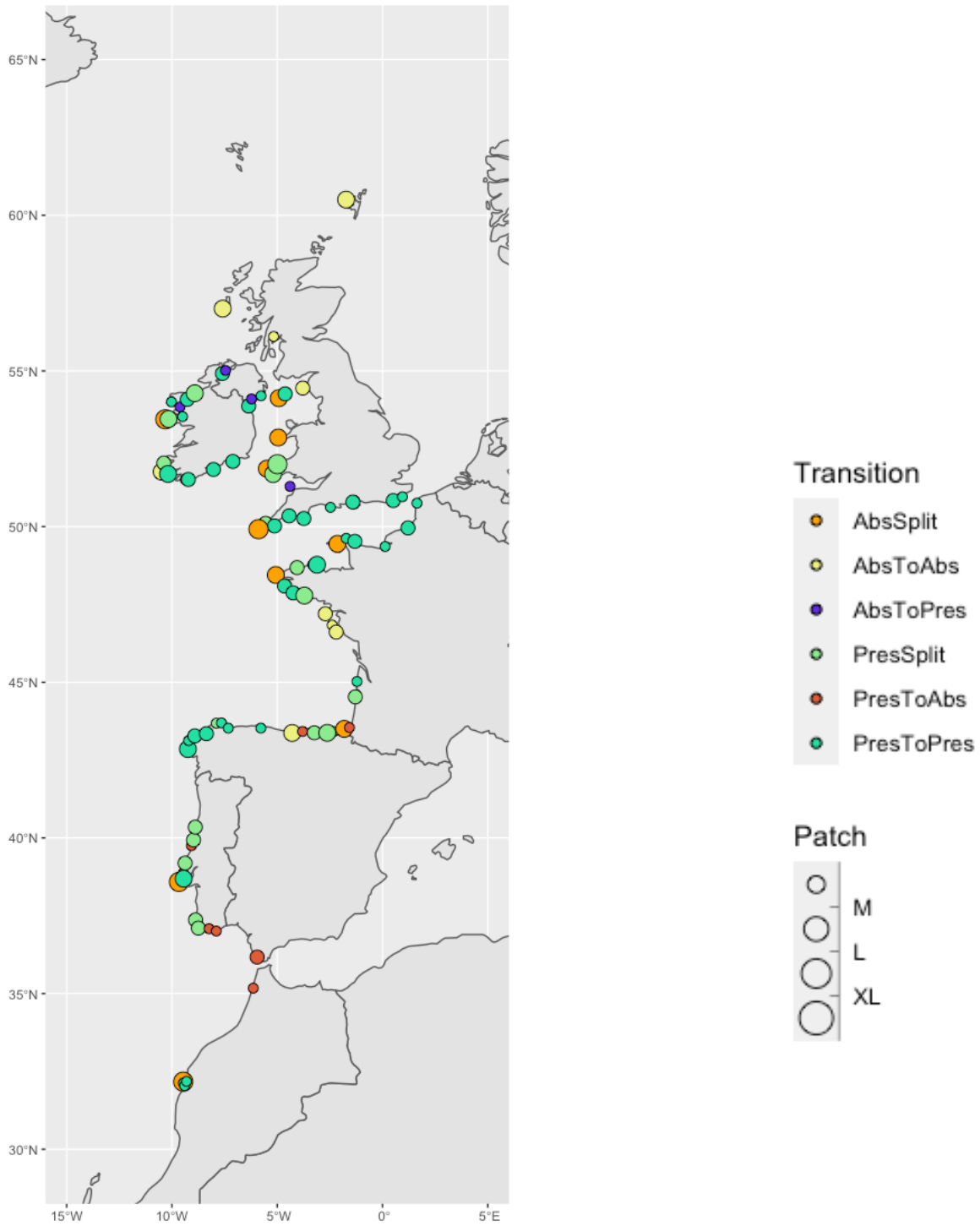


Figure S11. Variable response curves estimated under present-day conditions for all four algorithms used in the ensemble model. The average response (green line) and the associated confidence interval (grey area) were computed using predictions obtained from the 10 model runs and the 10 pseudo-absence datasets.



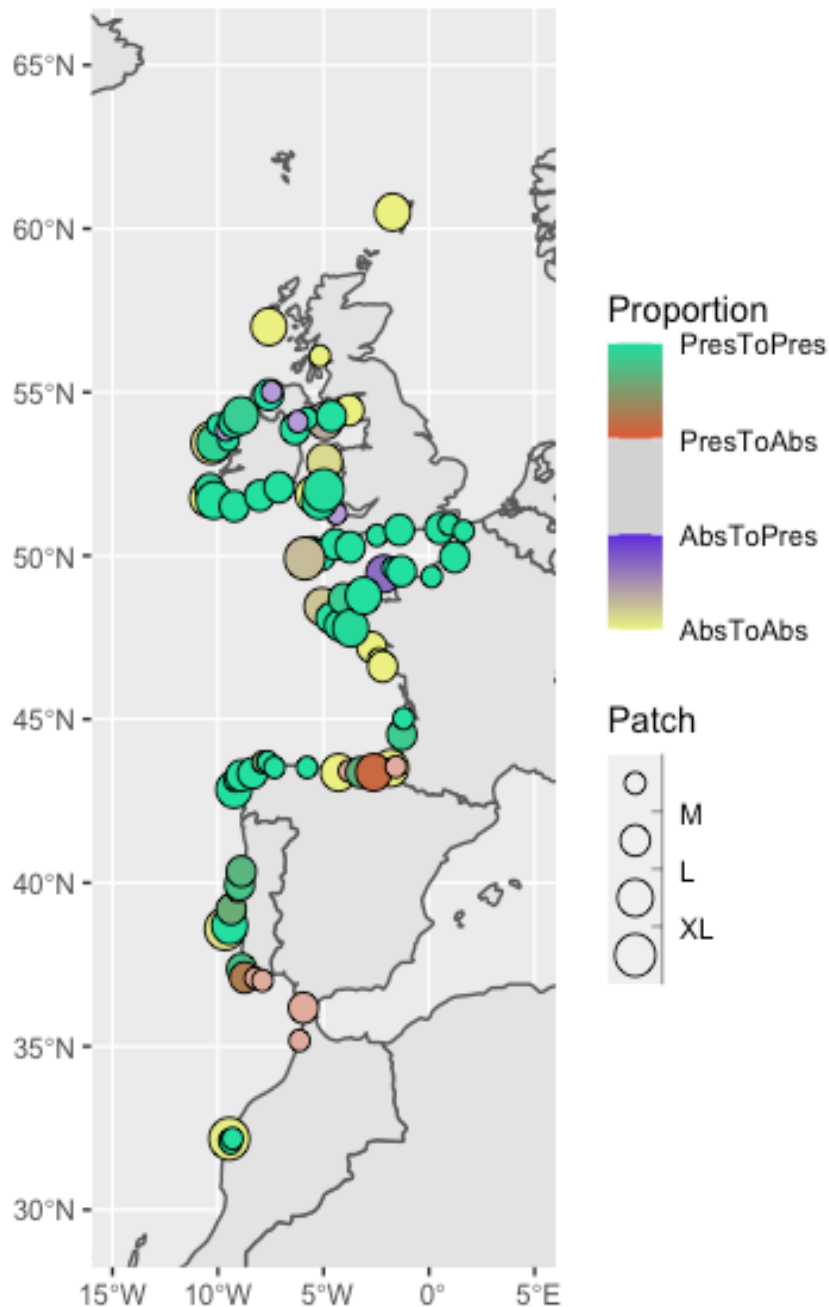
1 **Figure S12 (previous page).** Climate-driven patch-level changes across the latitudinal gradient.
2 Correspondence between the 90 patches of both presence (in green) and absence (in red) predicted
3 under current conditions, ordered along the x-axis by the latitudinal position of their poleward edge, and
4 the 92 patches predicted under future (RCP 4.5 2050) conditions, ordered along the y-axis. Bubbles
5 along the top and right-hand margins indicate patch size (log-scale). Groups of pixels changing between
6 presence and absence (in violet and orange) may form new patches in the future and reorganize the
7 spatial pattern of the species within the stable patches (in yellow and green). Deviations from the
8 diagonal indicate either presence patches expanding to form larger presence patches (Fig. 5b), absence
9 pixels appearing in patches of presence (extirpation; Fig. 5c), absence patches expanding to form larger
10 absence patches (Fig. 5d), or presence pixels colonizing patches of absence (Fig. 5e). An example of
11 each possibility is detailed in Figure 5.
12
13



14

15 **a**

16



17

18 **b**

19 **Figure S13.** Summary maps of predicted changes occurring to the 90 current patches under future
20 scenario RCP 4.5 by 2050. **a**, Categories reflect potential for no change (Persistence of 10 absence,
21 and 39 presence, patches), full shift from Absence to Presence (N=5) (or conversely Presence to
22 Absence; N=9), or partial shift (i.e. A patch becoming fragmented into both Absence and Presence
23 Patches in the future; N=10, or 17, for current absence, or presence, patches, respectively). **b**,
24 Continuous color scaling characterizing the proportion of fragmented patches shifting to Presence and
25 Absence in the future. Patches are located based on the latitudinal coordinates of their leading edge.
26 See Table S5 for a summary of all 90 patch transitions.

27

28

29

Table S1. Environmental predictors used for modelling the distribution of *Sabellaria alveolata*, including whether variables are used for present-day (**P**) or future predictions (**F**). Information on data sources, data resolution and time period, data type (RS: remote sensing; DO: direct observation; OM: ocean model; AM: atmospheric model) and data units is also provided.

Environmental predictor	Source	Resolution	Type	Units
P Wave fetch	<i>Burrows et al. 2020</i> ^a	0.0009°		
Summed wave fetch			OM	km
P/F Significant wave height (Hs)	<i>NOC wave model</i> ^b	0.083°		
		1975-2005		
Hs P90		2040-2050	DO, AOM	m
P/F Tidal amplitude	<i>OTIS-Regional Tidal Solution</i> ^c	0.083°		
Mean tidal amplitude (i.e. half the range)		1994-2011	OM	m
P/F Sea surface temperature (SST)	<i>Bio-ORACLE</i> ^{d,e}	0.083°		
		2000-2014		
Long-term SST min, mean, max		2040-2050	AOM	°C
P/F Sea surface salinity	<i>Bio-ORACLE</i> ^{d,e}	0.083°		

Mean Salinity	2000-2014		
	2040-2050	AOM	PSS
P/F Air temperature <i>WorldClim v1.4^f</i>	0.083°		
	1960-1990		
Annual mean temperature (BIO1)	2041-2060	AM	°C

30 ^a Burrows, M., 2020. Wave fetch GIS layers for Europe at 100m scale. figshare. Dataset.

31 <https://doi.org/10.6084/m9.figshare.8668127>

32 ^b Bricheno, L.M., Wolf, J., 2018. Future Wave Conditions of Europe, in Response to High-End Climate
33 Change Scenarios. *Journal of Geophysical Research: Oceans* 123, 8762–8791.

34 <https://doi.org/10.1029/2018JC013866>

35 ^c Egbert, G.D., Erofeeva, S.Y., Ray, R.D., 2010. Assimilation of altimetry data for nonlinear shallow-
36 water tides: Quarter-diurnal tides of the Northwest European Shelf. *Continental Shelf*

37 *Research* 30, 668–679. <https://doi.org/10.1016/j.csr.2009.10.011>

38 ^d Tyberghein, L., Verbruggen, H., Pauly, K., Troupin, C., Mineur, F., De Clerck, O., 2012. Bio-ORACLE:
39 a global environmental dataset for marine species distribution modelling: Bio-ORACLE marine
40 environmental data rasters. *Global Ecology and Biogeography* 21, 272–281.

41 <https://doi.org/10.1111/j.1466-8238.2011.00656.x>

42 ^e Assis, J., Tyberghein, L., Bosch, S., Verbruggen, H., Serrão, E.A., De Clerck, O., 2018. Bio-ORACLE
43 v2.0: Extending marine data layers for bioclimatic modelling. *Global Ecology and Biogeography*

44 27, 277–284. <https://doi.org/10.1111/geb.12693>

45 ^f Hijmans, R.J., Cameron, S.E., Parra, J.L., Jones, P.G., Jarvis, A., 2005. Very high resolution

46 interpolated climate surfaces for global land areas. *International Journal of Climatology* 25,

47 1965–1978. <https://doi.org/10.1002/joc.1276>

Table S2. Average (\bar{x}) and standard deviation of three SDM accuracy metrics (Kappa, TSS, AUC) computed across the 10 cross-validation runs, the 4 algorithms and the 10 pseudo-absence datasets.

	Testing data \bar{x}	Testing data SD	Sensitivity \bar{x}	Sensitivity SD	Specificity \bar{x}	Specificity SD
Kappa	0.468	± 0.05	0.515	± 0.054	0.953	± 0.063
TSS	0.673	± 0.05	0.887	± 0.053	0.784	± 0.063
AUC	0.910	± 0.03	0.887	± 0.056	0.785	± 0.065

48
49

Table S3. Variable importance per algorithm. For each variable, its importance was measured by computing 1 minus the correlation (Pearson's coefficient) between predictions obtained with the raw variable and predictions obtained with the same variable with randomized values. The larger the score, the larger the importance of the variable on model predictions.

	GAM	GLM	RF	BRT	\bar{x}
Fetch (FETCH)	0.317	0.416	0.251	0.412	0.349
Max. sea surface temperature					
(SST_MAX)	0.360	0.235	0.155	0.273	0.256
Mean salinity					
(SAL_MEAN)	0.137	0.194	0.105	0.085	0.130
Min. air temperature					
(AT_MIN)	0.176	0.186	0.072	0.026	0.115
90 th percentile Wave height					
(HS_P90)	0.135	0.104	0.126	0.041	0.102
Tidal amplitude					
(TIDE)	0.049	0.021	0.072	0.023	0.042

Pre-proof of Curd et al. 2023. Applying landscape metrics to species distribution model predictions to characterize internal range structure and associated changes. *Global Change Biology*, 29: 631-647. Please visit <https://onlinelibrary.wiley.com/doi/full/10.1111/gcb.16496> for final version.

Table S4. Metrics traditionally reported in SDM studies to document species range changes. Conversion from latitude to kilometers calculated with <https://www.nhc.noaa.gov/gccalc.shtml>

	Present (2000-2014)	Future (2040-2049)	Difference with current position (in latitude and kilometres)
Leading edge (Q95)	54.792N	55.542N	0.75 degree shift 83km shift poleward
Optimum/centroid	latitude 51.292N	latitude 51.292N	0 degree shift
Trailing edge (Q05)	37.404N	38.458N	1.054 degree shift 117km shift poleward

50
51

Table S5. Summary table of predicted changes occurring to the 90 current patches under future scenario RCP 4.5 by 2050. Categories reflect potential for no change (i.e. persistence of 10 absence patches, and 39 presence patches), total shift from Absence to Presence (N=5) or from Presence to Absence (N=9), and partial shift (i.e. a patch becoming fragmented into both Absence and Presence Patches in the future; N=10 or 17 for current absence, or presence, patches, respectively). Second row presents a similar summary of transition expressed as the proportion of all current patches.

	Absence	Absence	Presence	Presence	Absence -	Presence
	->	->	->	->	>	->
	Absence	Presence	Absence	Presence	Presence	Presence
					& Absence	& Absence
Absolute number of current patches per transition category	10	5	9	39	10	17
Proportion of current patches	0.11	0.06	0.10	0.43	0.11	0.19

52
53